

The effects of HIV Protease Inhibitors (Lopinavir/Ritonavir) on the non-oxidative pathways of glucose metabolism

by

Tarryn-Lee Fisher

Dissertation presented for the degree of Masters in Physiological Sciences in the
Faculty of Sciences at
Stellenbosch University



Supervisor: Professor M. Faadiel Essop

April 2014

Declaration

By submitting this thesis electronically, I declare that the entirety of the work contained therein is my own original work, that I am the sole author thereof (save to the extent explicitly otherwise stated), that reproduction and publication thereof by Stellenbosch University will not infringe any third party rights and that I have not previously in its entirety or in part submitted it for obtaining any qualification.

April 2014

Tarryn-Lee Fisher

Abstract (English)

While antiretroviral therapy decreases HIV/AIDS morbidity and mortality, long-term treatment results in insulin resistance and cardiovascular diseases. A possible cause of such adverse effects may be an increase in oxidative stress resulting from protease inhibitor (PI)-induced mitochondrial dysfunction. We therefore hypothesized that PI treatment, specifically Lopinavir/Ritonavir, results in increases in myocardial reactive oxygen species (ROS), leading to downstream outcomes, i.e. elevated apoptosis. Moreover, we proposed that increased ROS levels in this instance might occur as a result of PI-mediated induction of the non-oxidative glucose pathways (NOGPs). In light of this, we also investigated the effect of PI treatment on the NOGPs by employing both *in vitro* and *in vivo* samples. For the *in vitro* work we employed a rat cardiomyoblast cell line, while tissues (heart, liver) were collected from two separate experimental models, i.e. a) Group A exposed to PIs via mini-osmotic pump for a period of eight weeks, and b) Group B administered PIs via a jelly-based method for 16 weeks.

We found that PIs increased mitochondrial ROS levels *in vitro* but that this was not accompanied by a parallel rise in programmed cell death. Moreover, we found no induction of the NOGPs in response to PI exposure (for both *in vitro* and *in vivo* models here employed). However, we found that the AGE pathway was significantly down-regulated in the liver of Group A. Investigation into a proposed mechanism for this observation proved inconclusive and further studies are thus required to clarify the significance in terms of metabolic dysfunction found in the Group A model. Our study thus shows that PIs can increase ROS levels (*in vitro*) but that compensatory antioxidant

mechanisms may prevent this *in vivo*. Subsequently, downstream effects were limited i.e. we did not observe NOGP induction and programmed cell death. An intriguing finding emerged, however, i.e. that PIs can elicit an impact on the AGE pathway. We propose future studies with modifications to the current rat and cell models in order to evaluate the downstream effects of PIs on the NOGPs and programmed cell death.

Abstract (Afrikaans)

Terwyl antiretrovirale terapie MIV/VIGS morbiditeit en mortaliteit verlaag, veroorsaak langtermyn behandeling insulienweerstandigheid en kardiovaskulêre siekte. 'n Moontlike oorsaak van sulke nowe-effekte kan 'n toename in oksidatiewe stres veroorsaak deur die protease inhibeerder (PI)-geïnduseerde mitochondriale wanfunksionering. Ons hipotetiseer dat PI behandeling, spesifiek Lopinavir/Ritonavir, versoorsoak 'n toename in miokardiale reaktiewe suurstofspesies (ROS), wat aanleiding gee tot afstroom uitkomst, i.e. verhoogde apoptose. Verder, stel ons voor dat verhoogde ROS vlakke in hierdie geval ontstaan as gevolg van PI-gemedieerde induksie van die nie-oksidatiewe glukose weë (NOGWe). In die lig hiervan het ons ook die effek van PI behandeling op die NOGWe ondersoek deur beide *in vitro* en *in vivo* monsters te gebruik. Vir die *in vitro* werk het ons van 'n rot kardio-mioblastsellyn gebruik gemaak, terwyl weefsels (hart, lewer) versamel is van twee afsonderlike eksperimentele modelle, i.e. a) Groep A blootgestel aan PIs *via* mini-osmotiese pomp vir 'n periode van agt weke, en b) Groep B PIs is toegedien *via* 'n jellie gebaseerde metode vir 16 weke.

Ons het bevind dat die die PIs mitochondriale ROS vlakke *in vitro* verhoog maar dat dit nie vergesel is met 'n parallele toename in apoptose. Verder is geen induksie van die NOGWe in reaksie op PI blootstelling waargeneem (vir beide *in vitro* en *in vivo* modelle). Hoewel ons het bevind dat die AGE weg in die lewer van Groep A beduidend afgereguleer is. Ondersoek na 'n moontlike meganisme vir hierdie waarneming was onoortuigend en verdere ondersoek is nodig om die betekenis in terme van die metaboliese wanfunksionering in die Groep A model vas te stel. Ons studie toon dus aan

dat PIs, ROS vlakke (*in vitro*) verhoog, maar dat kompensatoriese anti-oksidant meganismes in die hierdie *in vivo* model verhoed word. Gevolglik is die afstroom effekte beperk i.e. ons het geen NOGWe induksie en apoptose waargeneem nie. 'n Interessante bevinding het wel uitgestaan, i.e. PIs kan 'n impak hê op die AGE weg. Ons stel dus voor dat toekomstige studies met modifikasies, tot die huidige rot- en sel-modelle gemaak word om die afstroomeffekte van PIs en apoptose te evalueer.

Acknowledgements

My sincere gratitude goes to my supervisor, Prof M. F. Essop. Your unwavering support, especially when things were at their very worst, made the world of difference. Thank you for having always been available with a sympathetic ear. Knowing that your door was always open for a chat, academic or otherwise, has helped me in more ways than you could imagine.

To the rest of CMRG, thank you for having accepted me into the group and for always having being willing to assist wherever needed. Special mention to Dr. Kathleen Reyskens and Dr. Danzil Joseph for their guidance and support.

For funding I would like to thank the NRF, as well as Dr. Theo Nel and Mr. Allan Forrester for financial contributions that were both much needed and much appreciated.

Lastly to my mother, Liesl Fisher, thank you for always being willing to support me and allowing me to fulfill my dreams (even if you didn't really understand what they were!). Your sacrifice has allowed me to go further than I would've ever thought possible. I love you and I am proud to be your daughter.

Tarryn-Lee Fisher

April 2014

"If we knew what it was we were doing, it would not be called research, would it?" - Albert Einstein

Table of Contents

List of Abbreviations	9
------------------------------	----------

List of Figures	12
------------------------	-----------

List of Tables	14
-----------------------	-----------

Chapter 1

Literature Review

<i>Introduction</i>	16
<i>The role of HIV infection in cardiovascular diseases</i>	18
<i>The development of HAART</i>	21
<i>Cardiovascular complications as a result of PI usage</i>	28
<i>The effect of PIs on metabolism</i>	30
<i>PI usage and the development of oxidative stress</i>	32
<i>The non-oxidative pathways of glucose metabolism</i>	37
<i>The effect of PIs on cell death</i>	51
<i>References</i>	57

Chapter 2

The effects of protease inhibitor (Lopinavir/Ritonavir) treatment on *in vitro* reactive oxygen species levels, programmed cell death and NOGPs

<i>Introduction</i>	74
<i>Materials & Methods</i>	76
<i>Results</i>	81
<i>Discussion</i>	84
<i>Conclusion</i>	86
<i>References</i>	87

Chapter 3

Analysis of the non-oxidative glucose pathways (NOGP) following protease inhibitor treatment (*in vivo* generated samples)

<i>Introduction</i>	91
<i>Materials & Methods</i>	92
<i>Results</i>	95
<i>Discussion</i>	100
<i>Conclusion</i>	102
<i>References</i>	103

List of Abbreviations

ACS	acute coronary syndrome
AGE	advanced glycation end product
AIDS	acquired immune deficiency syndrome
ANOVA	analysis of variance
AR	aldose reductase
ARI	aldose reductase inhibitor
ARV	antiretroviral
BSA	bovine serum albumin
CO ₂	carbon dioxide
CVD	cardiovascular diseases
DAG	diacylglycerol
DMEM	Dulbecco's Modified Eagle's Medium
DNA	deoxyribonucleic acid
eNOS	endothelial nitric oxide synthase
ER	endoplasmic reticulum
ETC	electron transport chain
F3P	fructose-3-phosphate
F6P	fructose-6-phosphate
FBS	fetal bovine serum

GAPDH	glyceraldehyde-3-phosphate dehydrogenase
GFAT	glutamine:fructose-6-phosphate-amidotransferase
GlucN-6-P	glucosamine-6-phosphate
GSH	glutathione
HAART	highly active anti-retroviral therapy
HBP	hexosamine biosynthetic pathway
HDL	high density lipoprotein
HIV	human immunodeficiency virus
IR	insulin resistance
LDL	low density lipoprotein
MetS	metabolic syndrome
MG	methylglyoxal
MI	myocardial infarction
NADH	nicotinamide adenine dinucleotide
NADPH	nicotinamide adenine dinucleotide phosphate
NNRTI	non-nucleoside reverse transcriptase inhibitor
NOGP	non-oxidative glucose pathways
NOX	nicotinamide adenine dinucleotide phosphate oxidase
NRTI	nucleoside reverse transcriptase inhibitor
<i>O</i> -GlcNac	<i>O</i> -linked N-acetylglucosamine
<i>O</i> -GlcNAcase	<i>O</i> -GlcNAc hexosaminidase

<i>O</i> -GlcNAcylation	<i>O</i> -linked <i>N</i> -acetyl-D-glucosaminylation
OGT	<i>O</i> -GlcNAc transferase
PARP	poly (adenosine diphosphate ribose) polymerase
PBS	phosphate-buffered saline
PI	protease inhibitor
PKC	protein kinase C
PUGNAc	<i>O</i> -[2-acetamido-2-deoxy-D-glucopyranosylidene]-amino- <i>N</i> -phenylcarbamate
ROS	reactive oxygen species
RNS	reactive nitrogen species
RT	reverse transcriptase
SEM	standard error of the mean
SOD	superoxide dismutase
T2DM	type 2 diabetes mellitus
TBS-T	Tris-buffered saline with Tween 20
TCA	tricarboxylic acid cycle
UDP-GlcNAc	uridine-5-diphosphate-N-acetylglucosamine

List of Figures

No table of figures entries found. **Chapter 1**

Fig. 1	The detrimental side effects of HIV infection <i>per se</i> and HAART	20
Fig. 2	HIV lifecycle and targets for ARVs	22
Fig. 3	The production of superoxide ($O_2^{\bullet-}$) by mitochondrial complex I and III	34
Fig. 4	Inhibition of GAPDH in the nucleus leads to activation of NOGPs, four potentially damaging alternate pathways to glucose metabolism	36
Fig. 5	The four non-oxidative pathways have damaging effects	37
Fig. 6	The polyol pathway is regulated by two enzymes	38
Fig. 7	The Maillard reaction	40
Fig. 8	Schematic representation of PKC activation	44
Fig. 9	The hexosamine biosynthetic pathway and protein <i>O</i> -GlcNAcation	47
Fig. 10	Cytochrome c and calcium regulation of apoptosis	52

Chapter 2

Fig. 1	Dose response curve to determine optimal PI dosage	81
Fig. 2	Apoptosis in rat-derived cardiomyoblasts in response to 24 hour PI treatment	82
Fig. 3	NOGP analysis in rat-derived H9c2 cardiomyoblasts following PI treatment	83

Chapter 3

Fig. 1 AGE pathway analysis in the rat heart and liver following PI treatment	96
Fig. 2 Polyol pathway analysis in the rat heart and liver following PI treatment	97
Fig. 3 HBP pathway analysis in the rat heart and liver following PI treatment	98
Fig. 4 PKC pathway analysis in the rat heart and liver following PI treatment	99

List of Tables

Chapter 1

Table 1 Adverse effects associated with different classes of ARVs 24

Table 2 Various cell and tissue types investigated for PI-induced
increases in ROS 32

Table 3 Protein *O*-GlcNAcylation modulates various processes 49

Chapter 2

Table 1 Antibody usage for Western Blotting analysis 79

Chapter 1

Literature Review

Introduction

The incidence of human immunodeficiency virus (HIV) infection has shown a dramatic increase over the past two decades. According to recent data released by UNAIDS the number of persons living with HIV in South Africa amounts to almost 6 million¹. While this number is alarmingly high, it does not vary much from the data collected by the World Health Organization in 2007². This indicates that the prevalence of the HIV/AIDS epidemic in South Africa is beginning to decrease, potentially attributed to improved access to highly active anti-retroviral therapy (HAART).

Although HAART increases the life expectancy of affected individuals, its long-term usage leads to various cardio-metabolic derangements, including cardiovascular diseases (CVD). Protease inhibitors (PIs) are an integral class of HAART with a variety of side-effects including the development of hyperlipidemia, hyperinsulinemia, hypertriglyceridemia and hypercholesterolemia³⁻⁵. PIs cause inflammation resulting in myocardial stress, which potentially predicts the onset of insulin resistance (IR) and cardiovascular abnormalities including myocardial infarction (MI) and CVD. Furthermore, PI-treated HIV-infected individuals show evidence of increased reactive oxygen species (ROS) production, which may activate harmful signaling and cell death pathways.

Unfortunately the underlying mechanisms for HAART-induced cardio-metabolic derangements are not well understood. Therefore our focus is to identify key metabolic pathways that mediate PI-induced cardio-metabolic pathophysiology. We hypothesize

that PIs induce the activation of the non-oxidative glucose pathways (NOGPs), resulting in a concurrent increase in ROS and subsequent cell death. This review will briefly focus on HIV infection and its potential contribution towards adverse cardio-metabolic perturbations, whereafter the emphasis will shift to the effects elicited by HAART. Here we will focus on especially the role of HIV-PIs and the potential role of particular metabolic circuits such as the NOGPs.

The role of HIV infection in cardiovascular diseases

The defining characteristic of HIV infection is that of a compromised immune system, ultimately leading to chronic, life-long inflammation and development of acquired immunodeficiency syndrome (AIDS). Prior to the development of HAART, various cardiac abnormalities were observed in HIV-infected patients, including dilated cardiomyopathy, endo-, myo- and peri-carditis, and pulmonary hypertension⁶⁻⁹. The direct effects of HIV on cardiac tissue is linked to the stages of HIV/AIDS infection¹⁰. Such effects will of course compound the negative prognosis and survival of HIV-infected individuals. Thus it is important to distinguish between the effects of antiretrovirals (ARVs) (focus of this thesis) and HIV infection *per se* in terms of the development of CVD and related abnormalities.

Various studies highlighted the challenge of chronic immune activation to the myocardium and the role of HIV in the development of CVD. For example, Becker *et al.*¹¹ found that HAART naïve HIV-infected patients with acute coronary syndrome (ACS) displayed less traditional risk factors for CVD than their HIV-negative counterparts with ACS. However, the thrombotic burden was significantly higher and angiographic characteristics altered. These findings were confirmed in similar studies^{12,13} and all data indicated the pathogenesis of CVD in HIV-infected individuals. HIV-infected individuals with ACS were compared to both HIV-negative and diabetic non-ACS individuals. Although all three groups displayed similar levels of multi-vessel disease, HIV-infected patients were significantly younger and had less complex lesions than their controls. Furthermore, the degree of subclinical coronary atherosclerosis was increased in the HIV-infected cohort¹³. Therefore it is evident that HIV itself is involved in viral-

mediated pathway activation that leads to the development of thrombotic and atherosclerotic disease infection, as well as the customary risk factor pathways.

With the advent of HAART, we are faced with the conundrum of co-morbidity, as now not only is HIV infection associated with an increased risk for future health complications, but long-term HAART usage can elicit side-effects such as increased cardiovascular complications¹⁴ (Figure 1). For example, HIV infection is associated with renal, vascular and pulmonary complications, more commonly associated with the geriatric population. Moreover, while HAART offers significant benefits in terms of the overall well-being of HIV-infected individuals, there are some concerns regarding side-effects.

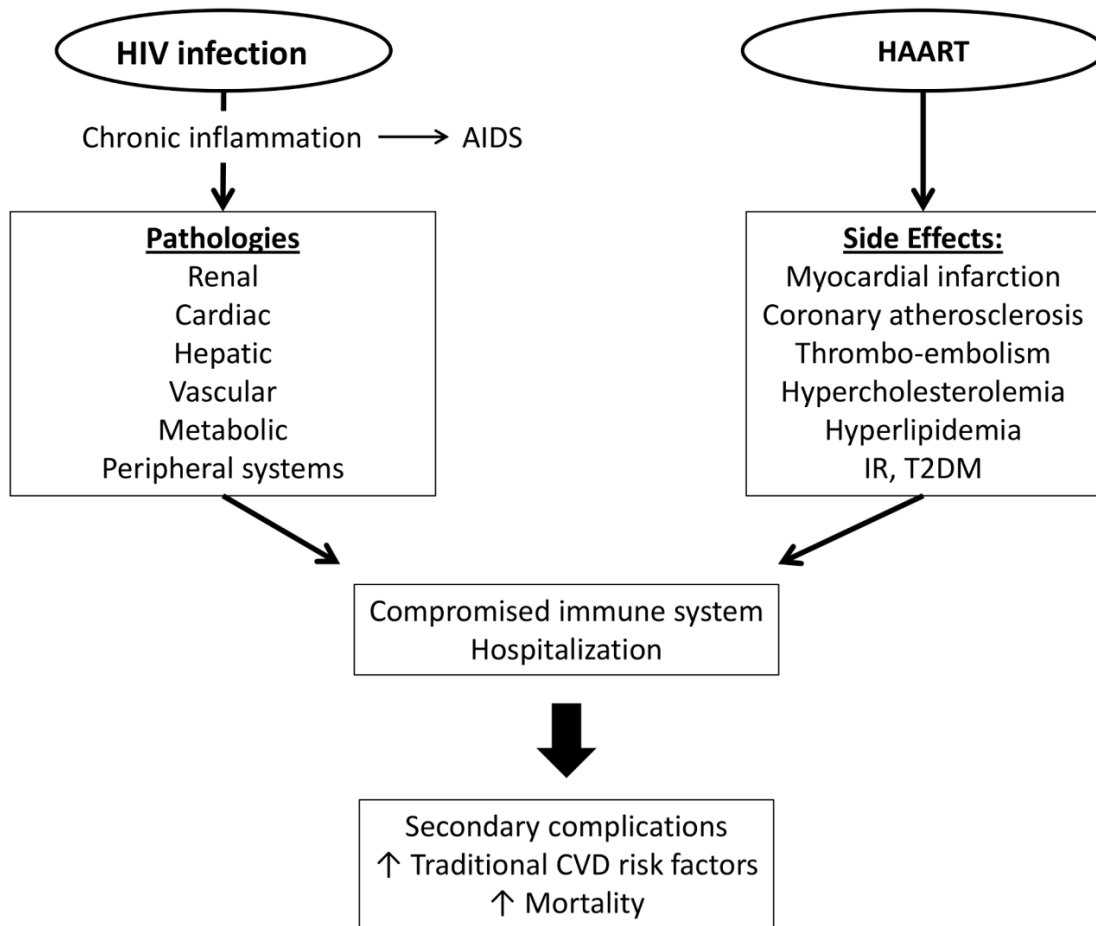


Figure 1. The detrimental side-effects of HIV infection *per se* and HAART¹⁵. Numerous organ systems can be negatively affected by HIV infection. While HAART dramatically decreases the HIV burden, it can also trigger a number of side-effects in some HIV-infected individuals. *IR* – *insulin resistance*, *T2DM* – *type 2 diabetes mellitus*.

The development of HAART

The advent of ARV usage sparked a noted increase in the life expectancy and quality of life of HIV-infected individuals, and has become essential tool to combat the devastating effects of HIV. The mechanism of action of ARVs is the inhibition of the viral life cycle at stages essential for proliferation of the virus (Figure 2). There are three distinct classes of ARVs which will be briefly discussed i.e. reverse transcriptase (RT) inhibitors (including non-nucleoside reverse transcriptase inhibitors [NNRTIs] and nucleoside reverse transcriptase inhibitors [NRTIs]), integrase inhibitors, and PIs.

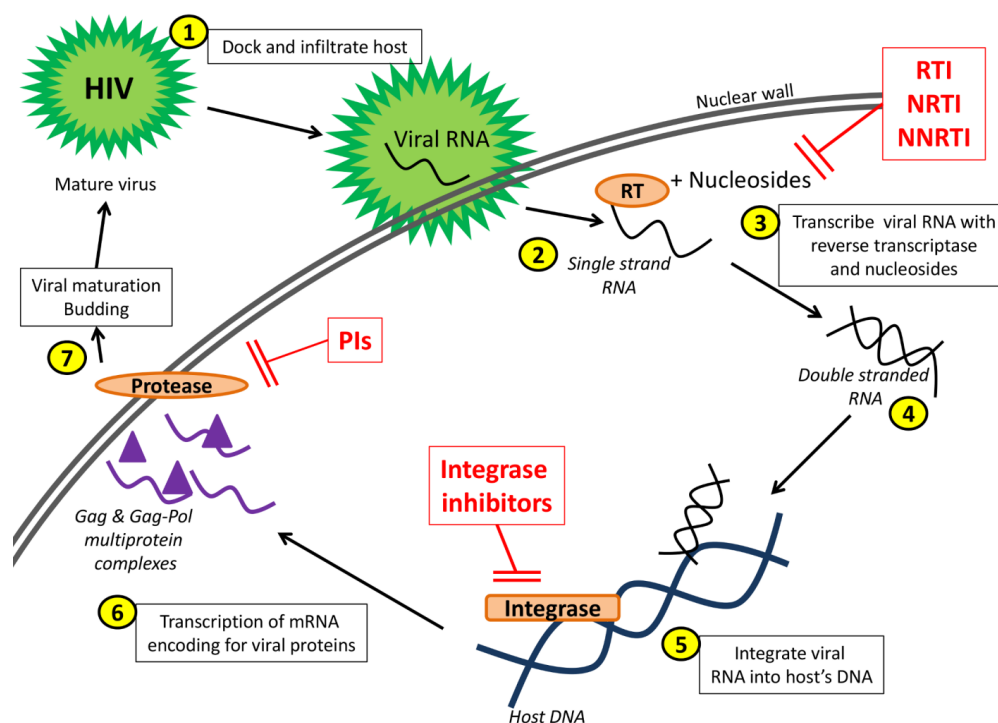


Figure 2. HIV lifecycle and targets for ARVs¹⁵. 1. The virus docks and infiltrates the host cell. 2. Single-strand viral RNA enters the host nucleus. 3. HIV RT and nucleosides transcribes single-stranded RNA. 4. Double-stranded RNA is produced which 5. Enters the nucleus and integrates itself within the host's DNA via HIV integrase. 6. Transcription allows viral mRNA production for viral proteins, 7. Gag and Gag-pol multi-protein complexes are formed and bud at the host's cell wall where proteases cleave proteins and mature viral particles. HAART can inhibit key viral enzymes at various stages of the viral life cycle. *RT* – reverse transcriptase, *NRTI*, *NNRTI* - nucleoside and non-nucleoside reverse transcriptase inhibitors, *PI* - protease inhibitors, *DNA* – deoxyribonucleic acid, *HIV* – human immunodeficiency virus, *mRNA* – messenger RNA, *RNA* – ribonucleic acid.

Reverse transcriptase inhibitors

RT inhibitors inhibit HIV-1 RT, an essential viral enzyme. Here this enzyme is responsible for the conversion of the positive single stranded RNA viral genome into double stranded DNA, which then becomes integrated into the host cell chromosomes¹⁶. RT is an appealing target for drug development as it is essential for HIV replication yet not required for host cell metabolism and thus has the potential to limit HIV-1 infection.

RT inhibitors can be divided into two classes: NRTIs and NNRTIs. NRTIs function by causing termination of DNA elongation via integration into newly synthesized DNA during reverse transcription. Elongation is disrupted due to chain terminators lack of the functional 3'-OH group required for the addition of nucleotides¹⁶. NNRTIs function by binding in a hydrophobic pocket next to the catalytic site of RT in HIV-1 and thereby inhibit viral replication¹⁷. While such inhibitors are effective in controlling viral proliferation in HIV-infected individuals, usage is often accompanied by a variety of adverse effects.

For example, medium- to long-term NRTI usage can cause inhibition of mitochondrial DNA polymerase γ , resulting in impairment of the synthesis of mitochondrial enzymes that generate ATP via oxidative phosphorylation¹⁸. A summary of the mitochondrial toxicities caused is shown in Table 1, with the severity of symptoms increasing with the duration of therapy. Adverse effects may also be exacerbated by underlying organ dysfunction, e.g. chronic liver disease, simultaneous HIV-1 opportunistic diseases, or via drug co-administration with similar toxicity profiles. NNRTIs display less severe side-effects and can elicit a positive effect on high density lipoproteins (HDL). For example, treatment with efavirenz causes elevated HDL levels, lowering the low density lipoprotein (LDL)/HDL cholesterol ratio and thus resulting in an improved lipid profile¹⁹.

Table 1: Adverse effects associated with different classes of ARVs³³

Class	Drug	Side effects
NRTIs	Zidovudine	Anemia, nausea, rash, myopathy, dyslipidemia
	Stavudine didanosine	Nausea, lipotrophy, DSPN, dyslipidemia, pancreatitis, lactic acidosis, hepatic streatosis, heart disease
	Abacavir	HSR, hepatotoxicity, heart disease
	Tenovir	Renal insufficiency, bone loss
NNRTIs	Efavirenz	CNS adverse effects, rash, hepatotoxicity, lipotrophy, teratogenicity
	Nevripine	Rash, HSR, hepatotoxicity
	Etravirine	Rash, hepatotoxicity
PIs	All PIs	Nausea, diarrhea, rash, dyslipidemia, IR, hepatotoxicity
	Atazanavir	Jaundice, scleral icterus, nephrolithiasis
	Indinavir	Jaundice, scleral icterus, nephrolithiasis
	Lopinavir fosamprenavir	Heart disease
Integrase inhibitors	Raltegravir	Headache, insomnia, dizziness, fatigue

DSPN - distal sensory peripheral neuropathy, HSR - hypersensitivity reactions, CNS – central nervous system, IR – insulin resistance

Integrase inhibitors

HIV integrase is responsible for the integration of the viral cDNA into the genome of infected cells and also acts as a cofactor for reverse transcription, and is therefore essential for viral replication²⁰. While integrase is necessary for viral proliferation, there is no host-cell equivalent and hence integrase inhibitors will not alter normal cellular processes. However, at relatively high doses (10-20 times higher than recommended) some integrase inhibitors can have an effect on recombinases required for normal antibody production²¹ as well as inhibiting RNase H²². This has been attributed to the structural similarities between integrases, recombinases and RNases²³.

Integrase inhibitors show the least adverse effects when compared to other drug classes (Table 1); however it is a relatively new ARV and limited long-term studies have yet been performed. However, naïve HIV-infected individuals treated for 24 weeks with raltegravir (in combination with tenofovir and lamivudine) displayed no significant changes for fasting serum cholesterol, LDL-cholesterol, HDL-cholesterol or triglyceride levels²⁴. To assess the effects of integrase inhibitors on their own the BENCHMRK (Blocking integrase in treatment Experienced patients with a Novel compound against HIV: MeRcK) trials were established. Results following a 96-week treatment period indicate similar side effects as previously reported²⁵.

Due to the low side-effect profile currently observed, patient adherence to the drug regimen might be higher than with other ARVs. This will then allow for future studies revealing long-term adverse effects as well as genetic influences with regard to drug resistance.

Protease inhibitors

More than 10 HIV PI-type drugs have been developed since the initiation of HAART in 1995²⁶. PIs function by acting as an inhibitor of HIV aspartyl protease, resulting in the production of immature, non-infectious viral particles²⁷, with no effect on cells already containing integrated viral DNA. PIs form an integral part of combination therapy, suppressing viral load and increasing CD4⁺ count, leading to decreased morbidity and mortality among HIV-infected individuals²⁸.

The development of combination ARVs represented an important step in the fight against HIV/AIDS. Often combination therapy consists of NNRTIs or PIs in conjunction with NRTIs, subsequently referred to as HAART. One such example of effective combination therapy is Lopinavir/Ritonavir, the latest PI developed, which forms part of second-line HAART in South Africa, and the focus of this study.

Kumar *et al.*²⁹ examined the metabolism of Lopinavir in various species and ascertained the maximal binding of this compound following uptake and release into circulation was to plasma proteins. They further discovered that Lopinavir was taken up by most tissues, albeit to varying degrees, including the rat heart.

Both Lopinavir and Ritonavir are heterocyclic compounds, with the liver the major site for Lopinavir metabolism i.e. by hepatic enzymes cytochrome P450 3A4 (CYP3A4) and cytochrome P450 3A5 (CYP3A5)³⁰, resulting in a number of oxidative metabolites although the main compound remains the major circulating drug. However, the circulating concentration of Lopinavir is insufficient to effectively suppress viral replication. Since Ritonavir is able to inhibit CYP3A4 and CYP3A5 thereby increasing

the plasma concentration of Lopinavir^{31,32}, a co-formulation drug was developed, i.e. Lopinavir/Ritonavir, also known as Kaletra™ or Aluvia™³¹.

PIs elicit an extensive side-effect profile (Table 1). It can cause gastrointestinal problems and metabolic abnormalities such as IR, hypertriglyceridemia and hypercholesterolemia. Since the focus of this study is on the cardio-metabolic effects of PIs, these topics will be covered more extensively in the next section.

Cardiovascular complications as a result of PI usage

PIs are associated with increased risk for myocardial infarction (MI) and coronary syndromes. For example, a large clinical study investigating the risk for MI with HAART, i.e. the Data Collection for Adverse events of Anti-HIV Drugs (DAD) Study group, recruited 23 468 HIV-infected patients on HAART³⁴⁻³⁶. Here accumulative exposure to HAART was linked to a significant increase in MI incidence, especially with PIs. In total 1.5 % of patients experienced MI. After adjusting for confounding parameters, the outright risk for MI was low although HAART and PIs increased normal CVD risk factors such as cholesterol and lipid abnormalities, and T2DM. Results from other studies followed a similar trend where the absolute risk of MI remains low^{37,38} but where PIs are associated with a significant increase in the occurrence of MI^{34,35,37-39}. Furthermore, increasing duration of HAART exposure, including PIs, can increase mortality and hospitalization for cardiovascular complications in the long term.

The use of Ritonavir, while boosting the efficacy of Lopinavir, also presents its own set of complications. For example, Ritonavir usage is associated with echocardiographic abnormalities, including significant rates of left ventricular systolic and diastolic dysfunction, as well as pulmonary hypertension and enlargement of the left atria⁴⁰. Thus while effective in their role as HIV suppressors, PIs specifically are associated with the onset of cardiovascular complications. However, the association between PI usage and atherosclerosis is also disputed, with some studies disregarding the link^{41,42} while others reveal a clear relation with the development of subclinical atherosclerotic lesions⁴³⁻⁴⁶ and thrombotic environments^{47,48}. Moreover, PIs are also strongly associated with the

development of increased risk for MI and coronary syndromes. Together this shows that HIV PIs are linked to the onset of cardiovascular complications and to various metabolic disorders, thereby triggering damaging effects at multiple levels.

The effect of PIs on metabolism

Metabolic perturbations can develop from PI usage, for example the metabolic syndrome (MetS), a culmination of risk factors predisposing the patient to the future onset of type 2 diabetes mellitus (T2DM) and CVD⁴⁹. While criteria for defining the MetS vary, the chief risk factors include abdominal obesity, atherogenic dyslipidemia, IR, raised blood pressure, pro-inflammatory status and pro-thrombotic state⁴⁹⁻⁵¹. Focusing on PI treatment, various studies based on cell-⁵²⁻⁵⁵, animal-⁵⁶⁻⁵⁸ and human-based⁵⁹⁻⁶⁵ models demonstrated increased plasma cholesterol and triglyceride levels, lipodystrophy and IR as the most common metabolic perturbations. Collectively these metabolic derangements can lead to the development of inflammation, which in turn can stress the myocardium and may eventually progress to cardiac dysfunction and also to the onset of IR^{63,66}. Thus this becomes a vicious metabolic cycle.

A variety of alterations to glucose metabolism were also found with PI usage, including the impairment of glucose tolerance. This includes whole-body glucose disposal, glucose uptake, transport and phosphorylation, as well as the development of IR at peripheral sites, e.g. skeletal muscle^{59,67,68}. Several studies found that IR is associated with PI usage even in the absence of apparent hyperglycemia⁶⁸. For example, Walli *et al.*⁶⁹ reported that the insulin sensitivity of HIV-infected individuals receiving PIs was significantly lower than control patients and HAART-naïve patients. Furthermore, a decrease in insulin sensitivity was also noted in HIV-negative patients receiving PI treatment. These results were confirmed in a similar study performed by Behrens *et al.*⁵⁸. While PI usage can elicit direct effects on the development of IR, the HIV virus itself

may also be implicated⁶⁸. Thus the picture that emerges is more complex and likely includes the effects of both PIs and the virus.

We therefore propose that, at the molecular level, PIs activate essential metabolic pathways to initiate a range of unfavorable alterations, which ultimately leads to the development of the above-mentioned metabolic derangements. Furthermore, these lipid- and glucose-mediated alterations may contribute to related pathophysiologies, i.e. an increase in oxidative stress, mitochondrial abnormalities, IR/T2DM and CVD.

PI usage and the development of oxidative stress

PI usage is correlated to increased reactive oxygen species (ROS) production and has been investigated by a number of studies utilizing human-⁷⁰, animal-^{71–74}, and cell-based^{75–79} models. Here a variety of tissue and cell types were investigated (Table 2) and the general consensus is that PI usage is linked to an increase in the production of oxidant species, as well as the activation of pro-oxidant pathways, which eventually leads to an increase in oxidative stress within such cells and tissues.

Table 2. Various cell and tissue types investigated for PI-induced increases in ROS

Author	Cell/Tissue type	Outcomes
Wang, X. <i>et al.</i> ⁷⁸ Lagathu, C. <i>et al.</i> ⁸⁰	Macrophages	Mitochondrial dysfunction, ↓cholesterol efflux, ↑ROS
Deng, W. <i>et al.</i> ⁸¹	Cardiomyocytes	↑ROS, ↑Cl ⁻ currents
Chai, H. <i>et al.</i> ⁸² Jiang, B. <i>et al.</i> ⁸³	Endothelial cells	↑endothelial mitochondrial dysfunction, ↑mtROS
Mondal, D. <i>et al.</i> ⁸⁴	Intestinal epithelial cells	↑mononuclear cell recruitment, ↑ROS
Wang, X. <i>et al.</i> ⁷⁷	Pulmonary aortic endothelial cells	↓eNOS synthase expression, ↑superoxide anion levels
Chandra, S. <i>et al.</i> ⁷⁴	Pancreatic β-cells	↑ROS, ↓cytosolic SOD
Touzet, O. & Phillips, A. ⁷⁵ Zaera, M. <i>et al.</i> ⁷¹	Human skeletal muscle cells	↑ROS, ↑mitochondrial respiratory chain dysfunction, ↑mtDNA deletions
Wang, X. <i>et al.</i> ⁷⁷	Porcine arteries	↓eNOS expression, ↑superoxide anion levels

eNOS – endothelial nitric oxide synthase, *mtROS* – mitochondrial ROS, *SOD* – superoxide dismutase, *mtDNA* – mitochondrial DNA.

However, intracellular ROS levels depend on both pro-oxidant systems and ROS-removal machinery. These systems cooperate to ensure optimal intracellular ROS levels at any given time.

ROS are formed intracellularly by cellular components, including the mitochondrial electron transport chain (ETC)^{85,86}, nicotinamide adenine dinucleotide phosphate oxidases (NOX)^{87,88}, xanthine oxidase^{89,90}, and cytochrome P450^{91,92}. However, while there are many ROS sources, its main producer is the mitochondrion, specifically via the ETC - either by respiratory chain complex I or complex III located within the inner mitochondrial membrane⁹³. ROS production begins by electrons being accepted from reducing equivalent molecules such as nicotinamide adenine dinucleotide/nicotinamide adenine dinucleotide phosphate (NADH/NADPH) and are passed into the ETC via mitochondrial respiratory complex I or III. Thereafter electrons are able to move through the ETC to the final electron acceptor in order to form water (H₂O) in complex IV. However, a few electrons can escape the system before encountering the final acceptor and can catalyze the monoelectronic reduction of molecular oxygen (O₂), to form superoxide (O₂^{•-}). Two pools of O₂^{•-} are created: firstly, O₂^{•-} generated by complex I in the inner mitochondrial membrane is released into the matrix where it is converted to hydrogen peroxide (H₂O₂) by manganese superoxide dismutase (MnSOD)^{87,93}, i.e. $2 \text{ O}_2^{\bullet-} + 2\text{H}^+ \rightarrow \text{O}_2 + \text{H}_2\text{O}_2$. Secondly, O₂^{•-} generated by complex III gets either shuttled into the mitochondrial matrix where it undergoes a similar fate as O₂^{•-} produced by complex I, or it is transferred to the inner mitochondrial membrane. Because the outer mitochondrial membrane is permeable to O₂^{•-}, it is able to translocate into the cytosol where copper/zinc superoxide dismutase (Cu/Zn SOD)

converts $O_2^{\bullet-}$ to H_2O_2 (Figure 3), which can be removed by glutathione peroxidase (GPx)

94,95

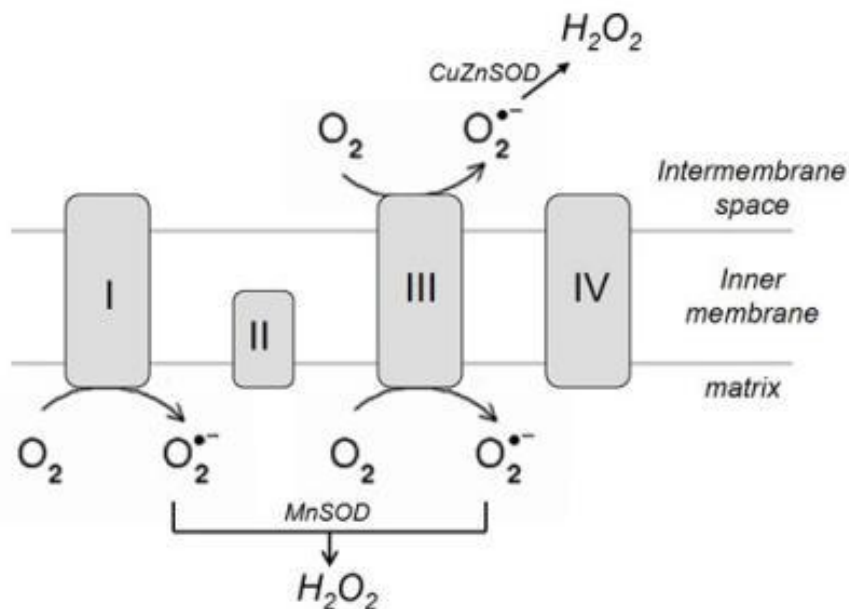


Figure 3. The production of superoxide ($O_2^{\bullet-}$) by mitochondrial complex I and III¹⁵. Free electrons leaked from the electron transport chain during oxidative respiration, allow for the formation of $O_2^{\bullet-}$ from molecular oxygen in complex I and III. $O_2^{\bullet-}$ generated from complex I gets converted to H_2O_2 by MnSOD in the mitochondrial matrix. $O_2^{\bullet-}$ generated by complex III undergoes a similar fate, but also gets translocated to the cytosol where it converted to H_2O_2 by Cu/Zn SOD. SOD – superoxide dismutase.

ROS is essential as a regulator of intracellular signaling pathways and gene expression under normal conditions referred to as “redox signaling”^{96,97}. NOX regulate the generation of $O_2^{\bullet-}$ generated by the transfer of an electron from NADH/NADPH to molecular oxygen^{98–101}. Generally the antioxidant defense system is sufficient to counteract the harmful effects of excessive ROS levels. However, when there is increased activation of ROS generating systems and/or when the antioxidant defense system is compromised then excess damaging ROS is produced. Here $O_2^{\bullet-}$ can react with nitric oxide to form peroxynitrite ($ONOO^-$), whereas H_2O_2 can be converted to a hydroxyl

anion (OH^\bullet) by non-enzymatic pathways, e.g. the Fenton reaction¹⁰². However, increases in ROS can also be due to adverse effects caused by PIs.

The origins, mechanisms and exact sequence of events for the production of PI-induced ROS are not well understood. While most studies suggest a mitochondrial origin¹⁰³, treatment of porcine carotid arteries with Ritonavir resulted in an increased endothelial nitric oxide synthase (eNOS)-generated production of $\text{O}_2^{\bullet-}$ ⁷⁹. This is indicative of an extra-mitochondrial ROS source. PI therapy is also responsible for alterations in functional mitochondrial biology e.g. increasing membrane potential depolarization in HL-1 myocytes⁸² and lowers cellular oxygen consumption¹⁰⁴.

For this study, we propose that there is a link between increased PI-mediated ROS generation and downstream activation of NOGPs. A rise in blood glucose levels leads to an increase in flux through the glycolytic pathway resulting in more glucose being oxidized by the tricarboxylic acid (TCA) cycle. Subsequently, more electrons pass through the ETC, increasing the proton gradient across the mitochondrial membrane¹⁰⁵. Complex III is blocked and electrons are trapped at co-enzyme Q from where it gets passed to O_2 , leading to an overproduction of $\text{O}_2^{\bullet-}$ ^{106,107}. Excess $\text{O}_2^{\bullet-}$ leads to DNA strand breakage and poly (adenosine diphosphate ribose) polymerase (PARP) is subsequently activated to repair such breaks¹⁰⁸. However, PARP also inhibits a key glycolytic enzyme glyceraldehyde-3-phosphate dehydrogenase (GAPDH), thus confining it to the nucleus¹⁰⁵. Consequently, glycolytic intermediates upstream of GAPDH are diverted into the NOGPs¹⁰⁹ (Figure 4).

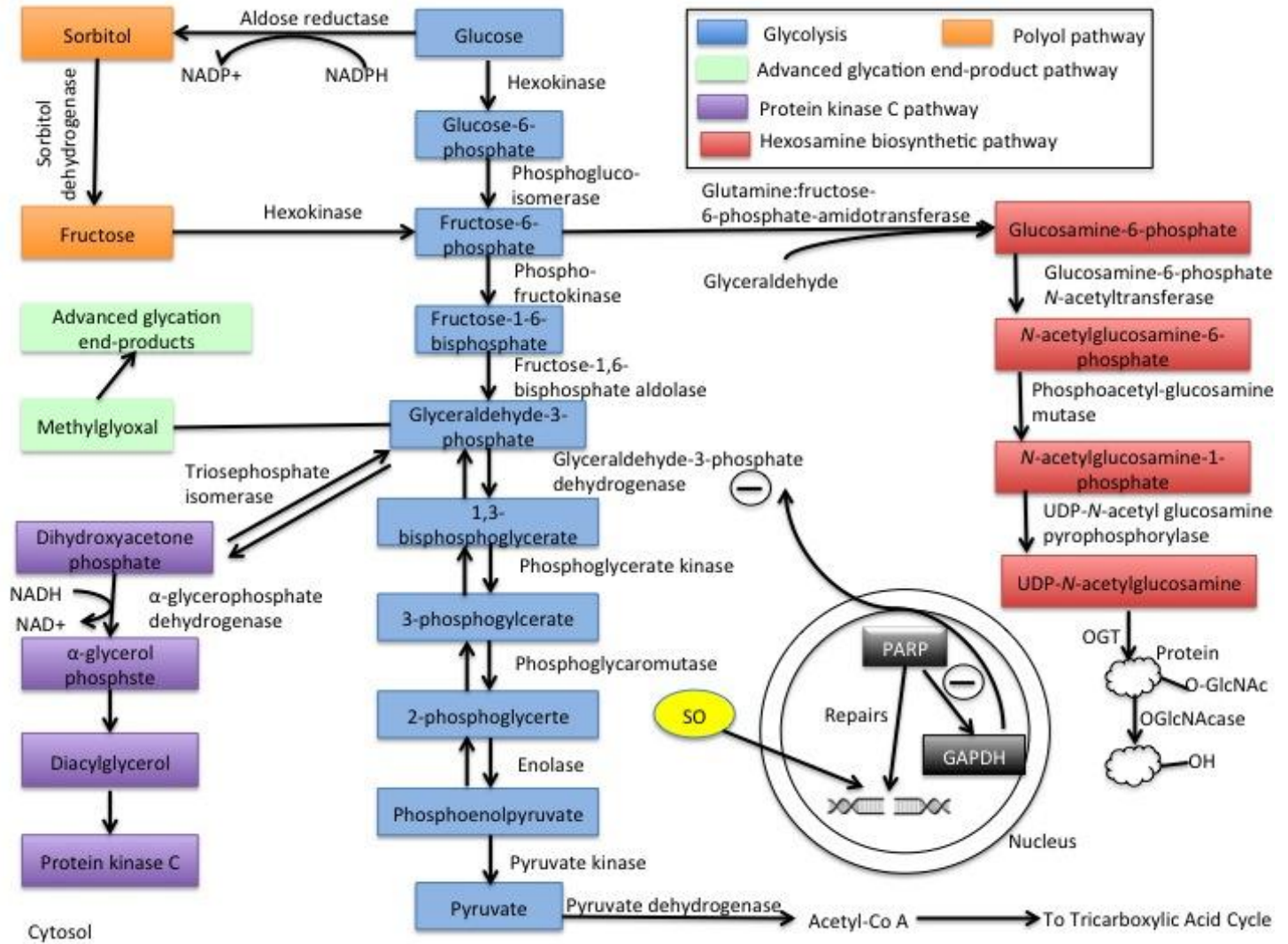


Figure 4. Inhibition of GAPDH in the nucleus leads to activation of NOGPs, four potentially damaging alternate pathways to glucose metabolism. PARP - poly (adenosine diphosphate ribose) polymerase, GAPDH - glyceraldehyde-3-phosphate dehydrogenase, SO – superoxide, OGT - O-GlcNAc transferase.

The non-oxidative pathways of glucose metabolism

There are four main pathways branching off from glycolysis which are implicated in microvascular and macrovascular complications arising from PI-induced hyperglycemia and ROS production, i.e. the polyol pathway, the formation of advanced glycation end-products (AGEs), activation of protein kinase C (PKC) and the hexosamine biosynthetic pathway (HBP). For this study, we propose that PI induced upregulation of NOGPs could occur and lead to subsequent complications (Figure 5).

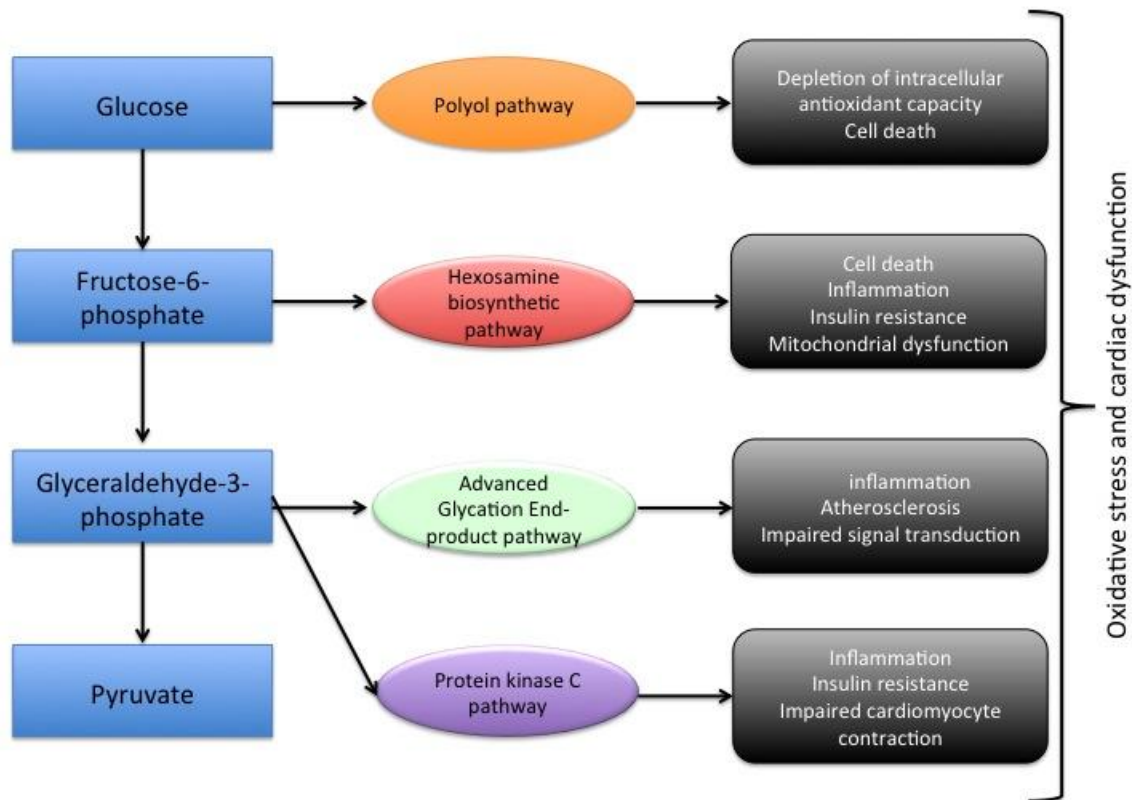


Figure 5. The four non-oxidative pathways have damaging effects. For this study, we propose that PI-induced upregulation of the NOGPs results in oxidative stress and cardio-metabolic abnormalities.

The polyol pathway

Increased flux through the polyol pathway is mediated by two enzymes i.e. aldose reductase (AR) and sorbitol dehydrogenase. Here AR together with its co-factor NADPH catalyzes the conversion of glucose to sorbitol, while sorbitol dehydrogenase (and its co-factor NAD⁺) allows for the conversion of sorbitol to fructose¹¹⁰ (Figure 6).

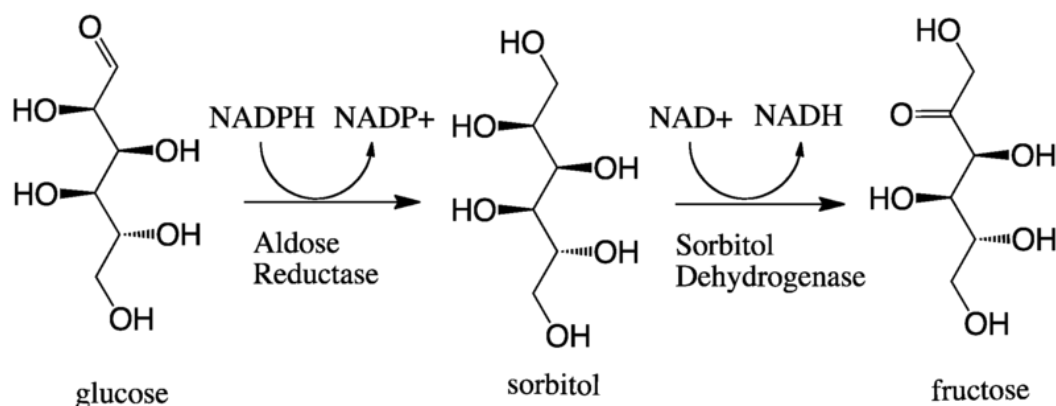


Figure 6. The polyol pathway is regulated by two enzymes. Aldose reductase and sorbitol dehydrogenase catalyze the conversion of glucose to fructose.

Three potential mechanisms for the contribution of the polyol pathway to oxidative stress exist. Firstly, increased AR activity may lead to the depletion of its co-factor NADPH, which is also required by glutathione (GSH) reductase to regenerate GSH. A decrease in GSH, an essential antioxidant in cells responsible for the eradication of various ROS species, may thus lead to increased ROS levels¹¹¹. The second mechanism involves the conversion of sorbitol to fructose, resulting in increased oxidative stress, as the co-factor for sorbitol dehydrogenase, NAD⁺, is converted to NADH. NADH is utilized as a substrate for NOX for ROS production¹¹². Lastly, increased polyol flux elevates the amount of fructose available that may be further metabolized to fructose-3-phosphate (F3P) and 3-deoxyglucosone, powerful nonenzymatic glycation agents, leading to

increases in AGEs. Therefore we hypothesize that PI-induced increases in flux through the polyol pathway can lead to increased ROS levels, resulting in a number of damaging effects.

Various pathologies associated with increased blood glucose are implicated with the formation of sorbitol. For example, Oates *et al.*¹¹³ performed animal model studies demonstrating that the utilization of AR inhibitors (ARI) prevented the development of diabetic complications. Furthermore, when diabetic rats were treated with ARIs, the GSH levels in the lens of the eye were higher than in untreated diabetic rats. Therefore AR activity causes oxidative stress¹¹⁴. However, sorbitol levels in neurons were not related to the severity of neural dysfunction¹¹⁵. This suggests that there may be other mechanisms involved in the development of diabetic lesions. For example, sorbitol accumulation-linked osmotic stress results in a loss of GSH, which may contribute to increased ROS^{116,117}.

Advanced glycation end-products

Proteins and lipids may become nonenzymatically glycosylated and oxidized subsequent to contact with aldose sugars, resulting in AGEs that are formed as a result of the Maillard reaction (Figure 7). Because glycation is concentration-dependent in the early stages of the Maillard reaction, it is heightened in diabetes¹¹⁸. The reaction begins with an initial glycation and oxidation event, resulting in the formation of Schiff bases and Amadori products, a 1-amino 1-deoxyketose, produced by the reaction of the carbonyl group of glucose with proteins, lipids and nucleic acids amino groups^{119,120}. Thereafter, Amadori reorganization occurs where carbonyl groups such as α -dicarbonyls or oxoaldehydes and

products that include 3-deoxyglucosone and methylglyoxal (MG) can accumulate^{121,122}.

This is known as “carbonyl stress” (Figure 7).

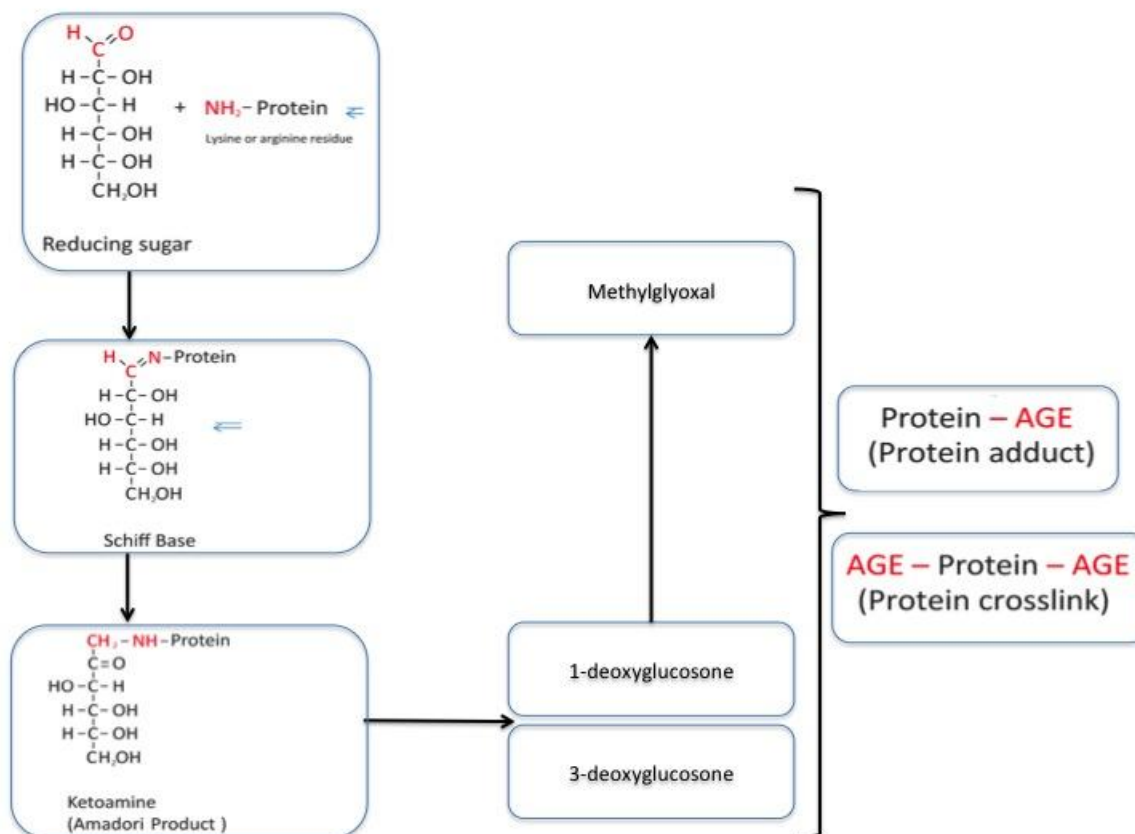


Figure 7. The Maillard reaction¹²³. Reducing sugars react with the amino group of proteins to produce a Schiff base. Molecular rearrangements result in more stable Amadori products. Further rearrangements, condensations and dehydrations result in the formation of intermediate α -oxoaldehydes such as methylglyoxal and 3-deoxyglucosone. Whether protein adducts or protein crosslinks are formed is dependent on the nature of early glycation events.

3-deoxyglucosone may also be formed from F3P, derived from the polyol pathway as discussed previously. Moreover, MG may also be formed via non-oxidative mechanisms in anaerobic glycolysis¹²⁴, and from the oxidative breakdown of polyunsaturated fatty acids¹²⁵. MG may also develop from fructose by fragmentation of triose phosphate or via the catabolism of ketone bodies and threonine¹²⁶. While such products may originate by

non-oxidative means, it can induce oxidative stress and cell death. For example, human monocytic leukemia cells showed increased apoptosis and oxidative stress when treated with varying concentrations of 3-deoxyglucosone and MG¹²⁷. A similar phenomenon was observed in rat Schwann cells¹²⁸, corticol neurons¹²⁹, and rat mesangial cells¹³⁰. The proposed mechanism for AGE-related apoptosis is via MG-mediated reduction of intracellular GSH and oxidative stress-mediated activation of the p38 mitogen-activated protein kinase (MAPK), an important kinase in cell death signaling¹³¹. Here the damaging effect of AGEs is evident and the variety of cell types affected is indicative of the scope of AGEs throughout the body.

There are three possible mechanisms for AGE-related damage: Firstly, the accumulation of AGEs in the extracellular matrix results in cross-link formation. This causes blood vessels to become narrower and stiffen, resulting in atherosclerosis which is further exacerbated by AGE interference with matrix-cell interactions and the modification of LDL cholesterol¹³². Secondly, AGE-mediated glycation of intracellular proteins may have an effect on signaling pathways. For example, intracellular AGEs reduce eNOS activity causing defective vasodilation and subsequent atherosclerosis¹³³. MG is a precursor of intracellular AGEs that modifies antioxidant systems resulting in increased oxidative stress. Lastly, the interaction of AGEs with their receptors (RAGEs) results in a downstream signaling cascade, leading to increases in ROS via activation of the NOX system¹³⁴.

While AGEs are implicated in numerous pathologies, including diabetic microvascular diseases, connective tissue diseases such as rheumatoid arthritis, neurological conditions such as Alzheimer's disease, and end-stage renal disease^{135–137}, it is not fully understood

whether it is the cause or effect of such conditions. For example, Raj *et al.*¹³⁸ performed an *in vitro* study that implicated AGEs as part of complex interactions with oxidative stress and vascular damage, e.g. the development of atherosclerosis. AGEs contribute to oxidative stress^{139,140} by inducing free-radical production and reducing nitric oxide concentrations¹⁴¹, resulting in vascular thickening with loss of elasticity, hypertension and endothelial dysfunction, as the vasodilatory and anti-proliferative effects of nitric oxide on vascular smooth muscle are eliminated¹⁴². In this case AGEs would be the cause of cardiovascular derangements. With Alzheimer's disease, however, there are increases in cerebral but not plasma AGEs, suggesting that AGE accumulation with Alzheimer's disease is a highly selective, brain specific event¹⁴³. Thus the conundrum remains whether AGEs are responsible for Alzheimer's disease or present as an effect of the disease.

The formation of AGEs is almost irreversible¹⁴⁴, although there is evidence that enzymes such as glyoxalase-1 are able to detoxify AGE precursors and inhibit AGE production^{119,145}. Both intracellular and extracellular proteins can be glycated and oxidized if certain factors are taken into consideration, i.e. the turnover rate of proteins for glycooxidation, the degree of hyperglycemia, and the extent of environmental oxidant stress^{119,144,146-148}.

The activation of protein kinase C

PKC forms part of a family of enzymes consisting of at least eleven different isoforms.

They are responsible for the transduction of signaling pathway cascades that stimulate the hydrolysis of lipids¹⁴⁹, the control of basic cell autonomous activities such as proliferation, and memory¹⁵⁰. PKC can be activated by diacylglycerol (DAG). DAG production is stimulated by activation of a large number of receptor families, including G protein-coupled receptors, tyrosine kinase receptors, and non-receptor tyrosine kinases. The process can be rapid e.g. by activation of specific phospholipase Cs, or more gradual by activation of phospholipase D. The latter results in the formation of phosphatidic acid and DAG production^{151–153}. Some PKCs can also be activated by calcium as they contain a calcium-binding site similar to calmodulin. PKCs activated by calcium interact with membrane acidic phospholipids, e.g. phosphatidylinositol. Calcium becomes available again after phospholipase C cleavage of phosphatidylinositol 4,5-bisphosphate into DAG and inositol 1,4,5-trisphosphate (IP₃). Thus multiple receptor pathways result in PKC activation by production of second messengers such as DAG and calcium (Figure 8).

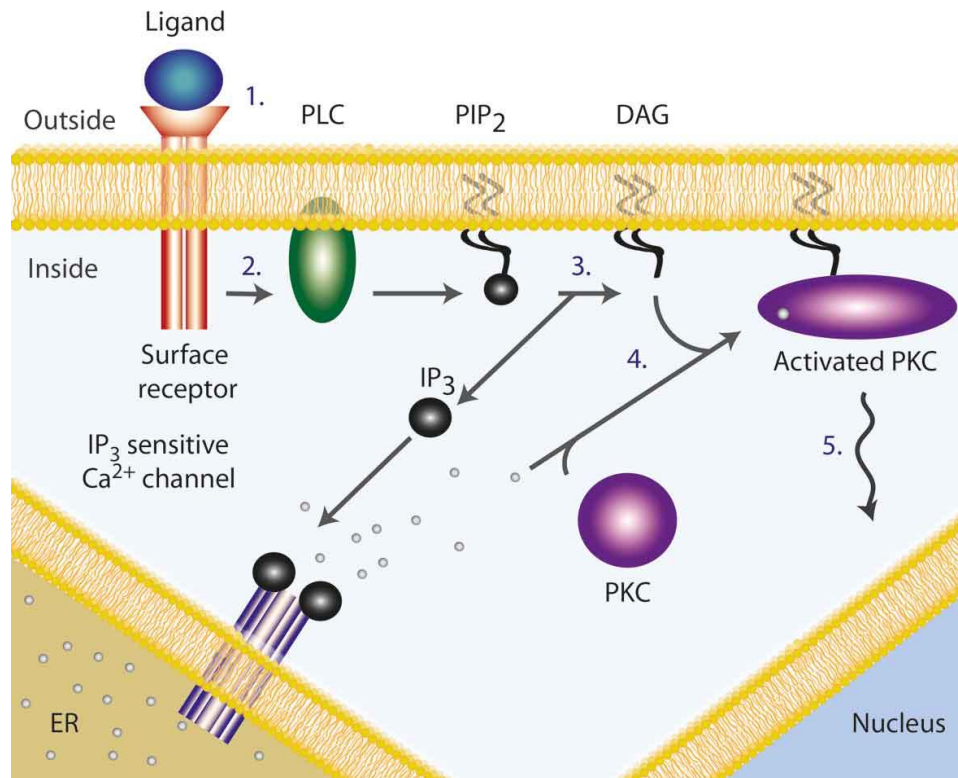


Figure 8. Schematic representation of PKC activation¹⁵⁴. 1. Ligand binding activates cell surface receptor which, 2. Activates PLC. 3. PLC cleaves PIP₂ into DAG and IP₃. 4. PKC is activated either by DAG or Ca²⁺ and undergoes a conformational change. 5. Activated PKC phosphorylates other cytosolic proteins. *PLC* – phospholipase C, *PIP₂* - Phosphatidylinositol 4,5-bisphosphate, *IP₃* - inositol 1,4,5-trisphosphate.

The mechanism of action of PKC is to phosphorylate serine or threonine residues in basic sequences¹⁵⁵. Unlike protein kinase A, it does so without the need for positive charge at specific positions and also with a lack of stereospecificity¹⁵⁶. PKC also possesses ATPase and phosphatase activities and is responsible for ATP hydrolysis by catalyzing a cofactor-dependent, substrate-stimulated reaction¹⁵⁷.

PKC is implicated in numerous processes throughout the body, including receptor desensitization, the mediation of immune responses, the regulation of membrane structure events, transcription and cell growth, as well as in learning and memory^{151–153,158,159}.

Because PKC is involved in the regulation of various vascular functions, it is plausible that the persistent PKC activation may result in numerous functional vascular anomalies in the diabetic patient. Moreover, with T2DM there is chronic activation of the DAG-PKC pathway in a variety of micro- and macro-vascular tissues^{160–165}. Subsequently, tissue DAG levels rise indicating that increased PKC activation with diabetes occurs as a result of a corresponding elevation in DAG levels.

A proposed mechanism for the glucose-activated increased DAG levels is attributed to greater *de novo* DAG synthesis. This can be simultaneously linked to diabetic vascular wall dysfunction, and is further substantiated by various studies utilizing PKC inhibitors^{165–170}. Elevated DAG *de novo* synthesis occurs due to increased formation of glucose metabolism precursors, e.g. dihydroxyacetone phosphate and glycerol-3-phosphate following stepwise acylation to lysophosphatidic acid and phosphatidic acid. The rate at which *de novo* DAG synthesis occurs is directly related to the amount of glucose available. Thus with hyperglycemia, *de novo* synthesis is enhanced because stimulation of phospholipid breakdown does not give preferentiality to glucose carbon incorporation into DAG¹⁷¹. Moreover, increases in saturated non-esterified fatty acids may also initiate the *de novo* synthesis of DAG and PKC activity and thereby increase ROS production.

ROS production by NOX may be responsible for various vascular abnormalities. For example, Inoguchi *et al.*¹⁷² found that an increase in glucose as well as treatment with PMA (a PKC activator) led to a significant increase in ROS in cultured aortic endothelial cells. Furthermore, when cells were subjected to diphenylene iodonium (a NOX inhibitor) and calphostin C (a PKC inhibitor), respectively, ROS levels decreased. These

data therefore suggest that elevated glucose levels resulted in increased ROS production via PKC-dependent activation of NOX.

The hexosamine biosynthetic pathway

Increased HBP flux (by way of excess glucose or free fatty acids) results in the formation of amino sugars. The pathway begins with fructose-6-phosphate (F6P) being converted to glucosamine-6-phosphate (GlucN-6-P) via the rate-limiting enzyme glutamine:fructose-6-phosphate-amidotransferase (GFAT), which makes use of glutamine as an amino donor^{173,174}. GFAT is also responsible for controlling the amount of glucose that enters the HBP and is therefore highly regulated. Regulation takes place via: 1. The concentration of F6P because affinity for the GFAT substrate is low; 2. Feedback inhibition of GFAT activity by uridine-5-diphosphate-N-acetylglucosamine (UDP-GlcNAc) through allosteric mechanisms¹⁷⁵; 3. GFAT activity is influenced by intracellular GFAT protein levels¹⁷⁶; and 4. GFAT activity is increased by 3',5' monophosphate (cAMP)-dependant phosphorylation¹⁷⁷. Thus GFAT inhibition prevents hyperglycemia-induced abnormalities e.g. IR and other diabetic complications^{174,178}.

The further conversion of GlucN-6-P results in the formation of UDP-GlcNAc, which is a precursor molecule for all other amino sugars necessary for multiple glycosylation reactions, resulting in the formation of glycoproteins, glycolipids, proteoglycans, and glycosaminoglycans¹⁷⁹ (Figure 9). Thus increased HBP activation results in a rise in *O*-linked *N*-acetyl-D-glucosaminylation (*O*-GlcNAcylation).

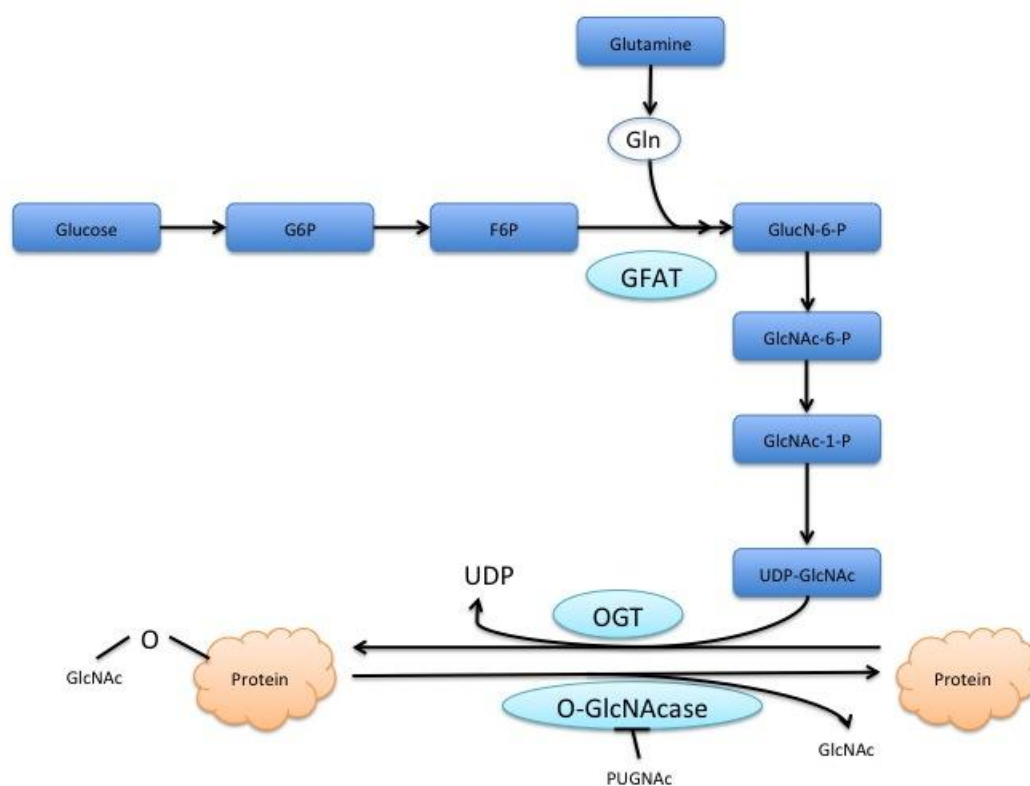


Figure 9. The hexosamine biosynthetic pathway and protein O-GlcNAcylation. F6P branches off from glycolysis and is converted to GlucN-6-P by GFAT, using glutamine as an amino donor. GlucN-6-P is converted to UDP-GlcNAc which allows for the addition of GlcNAc groups to proteins via OGT. The reaction is reversible via O-GlcNAcase. *OGT* - *O*-GlcNAc transferase, *O*-GlcNAcase - *O*-GlcNAc hexosaminidase, *PUGNAc* - *O*-[2-acetamido-2-deoxy-*D*-glucopyranosylidene]-amino-*N*-phenylcarbamate, *GlcNAc* - *N*-acetylglucosamine.

In eukaryotic cells a variety of nuclear and cytoplasmic proteins are modified at hydroxal groups of specific serine and threonine residues by *O*-linked N-acetylglucosamine (*O*-GlcNAc) moieties^{180,181}. The dynamic O-glycosidic linkage of GlcNAc to proteins is a reversible post-translational modification, differing from other glycosylation events as it takes place in the cytosol and nucleus¹⁸². The process of *O*-GlcNAcylation is catalyzed by *O*-GlcNAc transferase (OGT), with the reverse reaction under regulation of *O*-GlcNAc hexosaminidase (*O*-GlcNAcase)¹⁸³.

UDP-GlcNAc is the substrate for protein *O*-GlcNAcylation and can be synthesized in *de novo* fashion from glucose (via the HBP). Moreover, compounds such as glucosamine, streptozotocin, *O*-[2-acetamido-2-deoxy-D-glucopyranosylidene]-amino-*N*-phenylcarbamate (PUGNAc), and 2-deoxyglucose augment the process of *O*-GlcNAcylation by either increasing the availability of UDP-GlcNAc or via the inhibition of *O*-GlcNAcase^{184–186}. The effects of *O*-GlcNAcylation on proteins are varied across cell types and in terms of its end result on protein function (Table 3).

Table 3: Protein *O*-GlcNAcylation modulates various processes.

Modifications caused by <i>O</i>-GlcNAcylation	Outcomes
Enzyme activity	<ul style="list-style-type: none"> • Inhibition of eNOS^{187,188} • Reduced activation of glycogen synthase in IR¹⁸⁹
Protein-protein interactions	<ul style="list-style-type: none"> • Prevent untimely & ectopic interactions of Sp1¹⁹⁰ • Inhibits hydrophobic interactions between TAF110, holo-Sp1 and Sp1¹⁹¹ • Inhibits Sp1 transcriptional capability¹⁹²
DNA-binding affinity	<ul style="list-style-type: none"> • Regulation of PDX-1 DNA binding affinity & glucose-stimulated insulin secretion in β-cells¹⁹³
Subcellular localization	<ul style="list-style-type: none"> • Translocation of proteins from cytosol to nucleus e.g. eIF-1¹⁹⁴, La antigen¹⁹⁵, neoglycoproteins¹⁹⁶, glycoconjugates^{197,198}
Half life and proteolytic processing of proteins	<ul style="list-style-type: none"> • Protect eIF-2 α-subunit from eIF-2 kinase phosphorylation^{199,200} • Protects Sp1 from cAMP-mediated degradation²⁰¹ • Regulate transactivation & turnover of estrogen receptor β²⁰²

Studies by Du *et al.*²⁰³ on bovine aortic endothelial cells confirmed the involvement of hyperglycemia-induced increases in mitochondrial superoxide in terms of HBP activation.

This occurs via the inhibition of GAPDH activity, which diverts F6P from the glycolytic pathway and instead shuttles it into the formation of glucosamine. It can therefore be concluded that excessive HBP activation by hyperglycemia-induced mitochondrial superoxide overproduction may be responsible for derangements in both gene expression and protein function, leading to the development of diabetic complications. At the gene expression level, the exact mechanisms whereby increased HBP flux mediates hyperglycemia-induced gene expression are beginning to emerge. For example, Chen *et al*²⁰⁴ discovered that Sp1 sites regulate hyperglycemia-induced activation of the PAI-1 promoter in vascular smooth muscle cells and covalent modification of Sp1 by GlcNAc may explain the link. Furthermore, glycosylated Sp1 is more transcriptionally active than its de-glycosylated form, indicating that HBP flux has a direct effect on protein function.

To sum up, increased NOGP flux can elevate ROS levels with detrimental effects, e.g. cell death. Since we here propose that HIV-PIs can activate NOGPs, then this may provide a unique link between PIs and myocardial cell death.

The effect of PIs on cell death

Programmed cell death is a vital cellular process by which the integrity and homeostasis of multicellular organisms is maintained. Apoptosis is controlled by a variety of cell signals, which may be extracellular (extrinsic inducers) or intracellular (intrinsic inducers). Extracellular signals include toxins²⁰⁵, hormones²⁰⁶, growth factors²⁰⁷, nitric oxide²⁰⁸ and cytokines²⁰⁹, which must either cross the cell membrane or transduce in order to be effective. These signals can either induce or repress apoptosis. Intracellular signaling is brought about by the cell as a response to stress, e.g. glucocorticosteroid binding to nuclear receptors²⁰⁶, heat²¹⁰, radiation²¹¹, nutrient deprivation²¹², viral infection²¹³, hypoxia²¹⁴, and increased calcium concentrations²¹⁵.

Apoptosis is initiated in the mitochondrion and endoplasmic reticulum (ER), with the release of cytochrome c (from mitochondria) and calcium (from the ER) into the cytosol - as messengers for this process. In support, Boehning *et al.*²¹⁶ implicated calcium in the coordination of mitochondrial-ER interactions that drive apoptosis. Cytochrome c released from mitochondria in response to death signals binds to IP₃ receptors in the ER membrane, promoting calcium dispatch. This causes an increase in cytosolic calcium concentrations resulting in calcium uptake by mitochondria. The mass release of cytochrome c from mitochondria occurs at the same time. This allows for the formation and activation of an apoptosome (a protein complex that includes caspase and nuclease enzymes) that finalizes the apoptotic process (Figure 10).

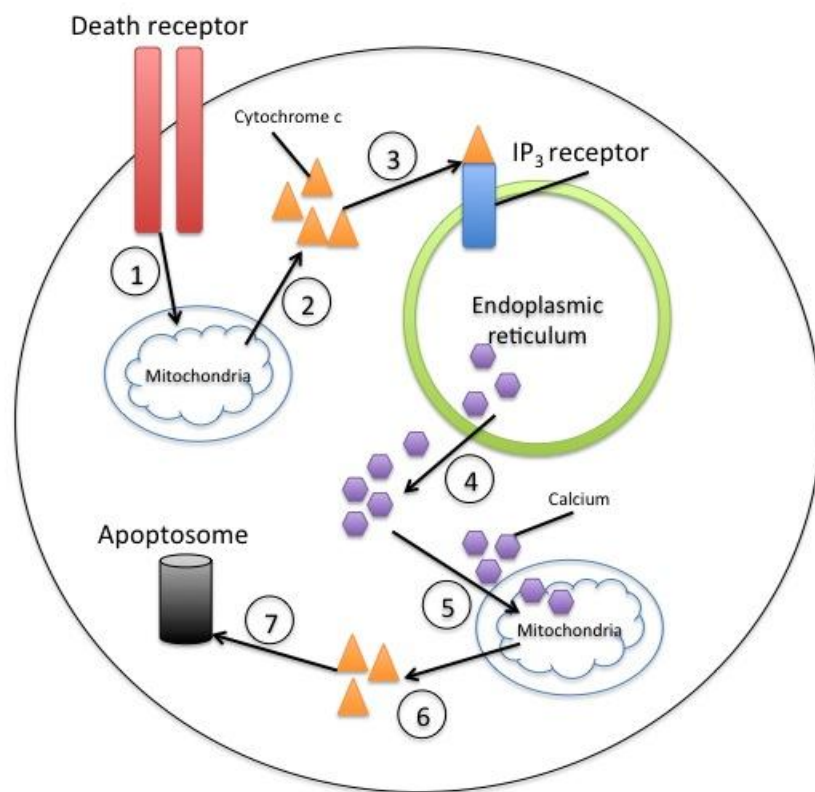


Figure 10. Cytochrome c and calcium regulation of apoptosis. 1. Death stimuli induce permeability transition in the mitochondrial membrane; 2. Cytochrome c is released from the mitochondrion into the cytosol; 3. Cytochrome c translocates to the ER and binds to the IP₃ receptor; 4. Calcium is released from the ER into the cytosol; 5. Calcium enters and stimulates adjacent mitochondria; 6. Mitochondria release cytochrome c; and 7. Cytosolic cytochrome c induces the formation of the apoptosome.

Since calcium is involved in many other cellular processes its role in apoptosis is strictly regulated. For example, after activation of IP₃ receptors the cytosolic anti-apoptotic transcription factor NF- κ B can be activated by a diffusible NF- κ B-activating factor that is released from the ER into the cytoplasm due to a decrease in intra-luminal calcium²¹⁷.

Deviations in this finely controlled process may manifest in various disease pathologies. For example, abnormal apoptosis can promote cancer development by allowing accumulation of dividing cells and by inhibiting removal of genetic variants with enhanced malignant potential²¹⁸. HIV/AIDS may be regarded as an imbalance between

CD4 cell death and cell replacement. Apoptosis was induced in HIV-infected MT2 lymphoblasts and activated normal peripheral blood mononuclear cells²¹⁹. This may be mediated by the HIV-1 gp120 glycoprotein which binds to the CD4 antigen since incubation of normal CD4 cells with HIV-1 gp120 followed by crosslinking causes apoptosis when stimulated by antibodies against the T-cell receptor antigen²²⁰.

For the purpose of this study we investigated the effects of PIs on cell death by means of death markers caspase 3, Bcl-2 and Bax, and pBAD. In light of this, these modulators will now be briefly discussed.

Caspase 3

Caspases, pro-apoptotic cysteine proteases, are essential for programmed cell death. Fourteen different caspases have thus far been identified in humans, each involved in inflammation and cell death. For the purpose of this study, caspase 3 levels were investigated as a key marker for apoptosis. In support, studies by Kuida *et al.*²²¹ and Woo *et al.*²²² on caspase-3-knockout mice validated the necessity of caspase 3 for survival. Further studies also elucidated the effects of caspase 3 in a variety of cell types in humans^{223,224}. Collectively these results are indicative of the involvement of caspase 3 in nuclear and morphological variations associated with the completion of apoptosis and the formation of apoptotic bodies.

The mechanism of caspase 3 action in the mediation of such variations is the cleavage of essential structural components, along with the incapacitation of critical homeostatic and repair processes²²⁵. The majority of caspase substrates are cleaved specifically by caspase 3, as well as pro-caspases 2, 6, 7 and 9, further confirming the extensive involvement of caspase 3 and related proteases in cell death^{225,226}.

HIV PI treatment can result in the inhibition of caspases^{227,228}. This is to be expected as HIV PIs are responsible for the inhibition of the aspartyl protease of HIV and would thus also have a similar effect on other cellular proteases.

Bcl-2 and Bax

Previous studies involving the nematode *Caenorhabditis elegans*²²⁹ revealed that the worm protein CED-9 is the functional homologue of Bcl-2²³⁰ and that it is responsible for the regulation of the activation of CED-3²³¹. Bcl-2 and its relatives are responsible for the regulation of the pathway that leads to the activation of caspases. It is induced by a variety of cellular stressors. Mammalian Bcl-2 has at least 20 relatives, all of which share at least one conserved Bcl-2 homology domain, and can be either pro- (e.g. Bax and BH3-only) or anti-apoptotic (e.g. Bcl-x_L, Bcl-w, A1 and Mc11). Members of the Bax family (promotes cell death) have sequences that overlap with the anti-apoptotic Bcl-2. Bcl-2 functions to inhibit apoptosis in response to certain cytotoxic events. This occurs by means of its hydrophobic carboxy-terminal domain, which aids in targeting Bcl-2 to the face of three intracellular membranes, i.e. the outer mitochondrial membrane, ER, and the nuclear envelope²³².

Bcl-2 is an essential membrane protein and Veis *et al.*²³³ found that it is crucial for every nucleated cell to have at least one Bcl-2 homolog present for its survival. This is the case since it is assumed that other anti-apoptotic proteins are not as effective in defending the cell against programmed cell death. Bax is widely distributed throughout the body and is thought to function mainly at the mitochondrion^{234,235}. In healthy cells it is present as a cytosolic monomer but it undergoes conformational changes during apoptosis, where it

integrates into the mitochondrial membrane and oligomerizes, resulting in mitochondrial dysfunction, cytochrome c release, activation of caspases, and ultimately cell death²³⁶.

pBAD

BAD is a member of the BH3-only, pro-apoptotic family of Bcl-2. Its activity is regulated by extracellular survival signals and it is phosphorylated and inactivated (by growth factors) at three serine residues: Ser-112, Ser-136, Ser-155^{237–239}. Phosphorylation of BAD is a reversible process so that in the absence of growth factors, it can bind to and deactivate Bcl-2, allowing for apoptosis to occur. When considering the context of HIV and HAART, studies done by Strack *et al.*²⁴⁰ confirmed the HIV-1 protease cleavage of Bcl-2, thereby increasing in apoptosis. However, no correlation could be found between PI treatment and an alteration in intracellular levels of anti-apoptotic markers such as Bcl-2²⁴¹.

Conclusion

HIV/AIDS remains a global epidemic despite a decrease in new infections. While various forms of HAART are available, they each present with their own adverse effects. This review demonstrates the damaging cardio-metabolic effects of PI treatment, e.g. long-term PI usage can result in the development of the MetS as well as a variety of CVD complications like atherosclerosis. Furthermore, PIs can increase ROS levels that could be detrimental to heart function. Finally, PIs can also induce hyperglycemia and IR that may be linked to even greater ROS production, with apoptosis as a putative end result. Thus while PIs significantly improve the life expectancy and quality of life of HIV-infected individuals, its long term usage can result in damaging cardio-metabolic side-effects. Moreover, mechanistic insights underlying such side-effects are not well understood especially in the heart. It is therefore imperative that further research be done in this field to help improve future drug design and lighten the disease burden of those already infected with HIV/AIDS.

We therefore hypothesize that PIs can alter the flux through the NOGPs leading to increased ROS production and apoptosis. The aim of this study was thus to assess the production of mitochondrial ROS following PI treatment, as well as to establish whether induction of NOGPs occurs and whether there is any correlation of the latter to increases in cell death.

References

1. UNAIDS. *2011 UNAIDS World AIDS Day report, Sub-saharan Africa*. 0–2 (2011).
2. UNAIDS. *UNAIDS/WHO Epidemiological Fact Sheets on HIV and AIDS, 2008 Update*. 4 (2008).
3. Safrin, S. & Grunfeld, C. Fat distribution and metabolic changes in patients with HIV infection. *AIDS* **13**, 2493–2505 (1999).
4. Carr, A. *et al.* A syndrome of peripheral lipodystrophy, hyperlipidaemia and insulin resistance in patients receiving HIV protease inhibitors. *AIDS* **12**, F51–58 (1998).
5. Carr, A. *et al.* Diagnosis, prediction, and natural course of HIV-1 protease-inhibitor-associated lipodystrophy, hyperlipidaemia, and diabetes mellitus: a cohort study. *Lancet* **353**, 2093–2099 (1999).
6. Himelman, R. B., Chung, W. S., Chernoff, D. N., Schiller, N. B., & Hollander, H. Cardiac manifestations of human immunodeficiency virus infection: a two-dimensional echocardiographic study. *J Am Coll Cardiol* **13**, 1030–1036 (1989).
7. Hecht, S., Berger, M., Van Tosh, A., & Croxson, S. Unsuspected cardiac abnormalities in the acquired immune deficiency syndrome. An echocardiographic study. *Chest* **96**, 805–808 (1989).
8. Kaul, S., Fishbein, M., & Siegel, R. Cardiac manifestations of acquired immune deficiency syndrome: a 1991 update. *Am Heart J* **122**, 535–544 (1991).
9. Rerkpattanapipat, P., Wongpraparut, N., Jacobs, L. E., & Kotler, M. N. Cardiac manifestations of acquired immunodeficiency syndrome. *Arch Int Med* **160**, 602–608 (2000).
10. Grody, W. W., Cheng, L. & Lewis, W. Infection of the heart by the human immunodeficiency virus. *Am J Cardiol* **66**, 203–206 (1990).
11. Becker, A. *et al.* Acute coronary syndromes in treatment-naïve black South Africans with human immunodeficiency virus infection. *J Interv. Cardiol* **23**, 70–77 (2010).
12. Knudsen, A. *et al.* Angiographic features and cardiovascular risk factors in human immunodeficiency virus-infected patients with first-time acute coronary syndrome. *Am J Cardiol* **111**, 63–67 (2013).
13. Lo, J. *et al.* Increased prevalence of subclinical coronary atherosclerosis detected by coronary computed tomography angiography in HIV-infected men. *AIDS* **24**, 243–253 (2010).
14. Goulet, J. L. *et al.* Do patterns of comorbidity vary by HIV status, age, and HIV severity? *Clin Infect Dis* **45**, 1593–1601 (2007).
15. Reyskens, K. M. S. E. The Maladaptive Effects of HIV Protease Inhibitors (Lopinavir/Ritonavir) on the Rat Heart. 27 (2013).
16. Tantillo, C. *et al.* Locations of Anti-AIDS Drug Binding Sites and Resistance Mutations in the Three-dimensional Structure of HIV-1 Reverse Transcriptase. *J Mol Biol* **243**, 369–387 (1994).

17. Pedersen, O. S. & Pedersen, E. B. Non-nucleoside reverse transcriptase inhibitors: the NNRTI boom. *Antivir. Chem. Chemother.* **10**, 369–387 (1999).
18. Carr, A. & Cooper, D. A. Adverse drug reactions Adverse effects of antiretroviral therapy. *Lancet* **356**, 1423–1430 (2000).
19. Negredo, E. *et al.* Efavirenz induces a striking and generalized increase of HDL-cholesterol in HIV-infected patients. *AIDS* **18**, 819–821 (2004).
20. Zhu, K., Dobard, C. & Chow, S. A. Requirement for integrase during reverse transcription of human immunodeficiency virus type 1 and the effect of cysteine mutations of integrase on its interactions with reverse transcriptase. *J Virol* **78**, 5045–5055 (2004).
21. Melek, M. *et al.* Effect of HIV integrase inhibitors on the RAG1/2 recombinase. *Proc. Natl. Acad. Sci. U. S. A.* **99**, 134–7 (2002).
22. Shaw-Reid, C. a *et al.* Inhibition of HIV-1 ribonuclease H by a novel diketo acid, 4-[5-(benzoylamino)thien-2-yl]-2,4-dioxobutanoic acid. *J. Biol. Chem.* **278**, 2777–80 (2003).
23. Rice, P. A. & Baker, T. A. Comparative architecture of transposase and integrase complexes. *Nat. Struct. Biol.* **8**, 302–307 (2001).
24. Teppler, H., Azrolan, N., Chen, J. & Nguyen, N. Y. *Differential effect of MK-0518 and efavirenz on serum lipids and lipoproteins in antiretroviral therapy (ART)-naïve patients. 46th Intersci. Conf. Antimicrob. Agents Chemother.* 27–30 (2006).
25. Steigbigel, R. T. *et al.* Long-term efficacy and safety of Raltegravir combined with optimized background therapy in treatment-experienced patients with drug-resistant HIV infection: week 96 results of the BENCHMRK 1 and 2 Phase III trials. *Clin. Infect. Dis.* **50**, 605–12 (2010).
26. Chandwani, A., & Shuter, J. Lopinavir/ritonavir in the treatment of HIV-1 infection: a review. *Ther. Clin Risk Man* **4**, 1023–1033 (2008).
27. Debouck, C. The HIV-1 protease as a therapeutic target for AIDS. *AIDS Res Hum Retrovir* **8**, 153–164 (1992).
28. Flexner, C. HIV Protease Inhibitors. *N. Engl. J. Med.* **338**, 1281–1292 (1998).
29. Kumar, G. N. *et al.* Metabolism and disposition of the HIV-1 protease inhibitor lopinavir (ABT-378) given in combination with ritonavir in rats, dogs, and humans. *Pharm. Res* **21**, 1622–1630 (2004).
30. Kaplan, S. S., & Hicks, C. B. Safety and antiviral activity of lopinavir/ritonavir-based therapy in human immunodeficiency virus type 1 (HIV-1) infection. *Antimicrob Chemother* **56**, 273–276 (2005).
31. Hsu, A., Granneman, G. R. & Bertz, R. Ritonavir. Clinical pharmacokinetics and interactions with other anti-HIV agents. *Clin Pharmacol* **35**, 275–291 (1998).
32. Mondy, K. E. *et al.* High prevalence of echocardiographic abnormalities among HIV-infected persons in the era of highly active antiretroviral therapy. *Clin Infect Dis* **52**, 378–386 (2011).

33. Hawkins, T. Understanding and managing the adverse effects of antiretroviral therapy. *Antiviral Res.* **85**, 201–9 (2010).
34. Friis-Møller, N. *et al.* Cardiovascular disease risk factors in HIV patients--association with antiretroviral therapy. Results from the DAD study. *AIDS* **17**, 1179–93 (2003).
35. Friis-Møller, N. *et al.* Class of antiretroviral drugs and the risk of myocardial infarction. *N. Engl. J. Med.* **356**, 1723–35 (2007).
36. Smith, C. *et al.* Factors associated with specific causes of death amongst HIV-positive individuals in the D:A:D Study. *AIDS* **24**, 1537–48 (2010).
37. Holmberg, S. D. *et al.* Protease inhibitors and cardiovascular outcomes in patients with HIV-1. *Lancet* **360**, 1747–1748 (2002).
38. Mary-Krause, M., Cotte, L., Simon, A., Partisani, M. & Costagliola, D. Increased risk of myocardial infarction with duration of protease inhibitor therapy in HIV-infected men. *AIDS* **17**, 2479–86 (2003).
39. Durand, M., Sheehy, O., Baril, J.-G., Leloirier, J. & Tremblay, C. L. Protease inhibitors and cardiovascular outcomes in patients with HIV-1. *J AIDS* **57**, 245–53 (2011).
40. Sullivan, P. S., Dworkin, M. S., Jones, J. L. & Craig, W. Epidemiology of thrombosis in HIV-infected individuals. *AIDS* **14**, 321–324 (2000).
41. Lyonne, L. *et al.* Thromboembolic events at the time of highly active antiretroviral therapies against human immunodeficiency virus. *Rev Med Intern* **29**, 100–104 (2008).
42. Jerico, C. *et al.* Subclinical carotid atherosclerosis in HIV-infected patients: a role of combination antiretroviral therapy. *Stroke* **37**, 812–817 (2006).
43. De Saint Martin, L. *et al.* Premature atherosclerosis in HIV positive patients and cumulated time of exposure to antiretroviral therapy (SHIVA study). *Atherosclerosis* **185**, 361–367 (2006).
44. Maggi, P., Lillo, A., Perilli, F. & Maserati, R. Colour-doppler ultrasonography of carotid vessels in patients treated with antiretroviral therapy: a comparative study. *AIDS* **18**, 1023–1028 (2004).
45. Bernal, E. *et al.* Hypertriglyceridemic waist phenotype is a risk factor for subclinical atherosclerosis in human immunodeficiency virus-infected patients. *Med Clin* **139**, 561–565 (2012).
46. Lijfering, W. M., Ten Kate, M. K., Sprenger, H. G. & van der Meer, J. Absolute risk of venous and arterial thrombosis in HIV-infected patients and effects of combination antiretroviral therapy. *J Thromb Haemost* **4**, 1928–1930 (2006).
47. Majluf-Cruz, A. *et al.* Venous thrombosis among patients with AIDS. *Clin Appl Thromb Hemostas* **10**, 19–25 (2004).
48. Grundy, S. M., Brewer, H. B., Cleeman, J. I., Smith, S. C. & Lenfant, C. Definition of metabolic syndrome: report of the National Heart, Lung, and Blood Institute/American Heart Association conference on scientific issues related to definition. *Circulation* **109**, 433–438 (2004).
49. Reaven, G. *The metabolic syndrome*. 11–36 (Humana Press, 2008).

50. Third report of the National Cholesterol Education Program (NCEP) expert panel on detection, evaluation, and treatment of high blood cholesterol in adults (Adult Treatment Panel III). Final report. *Circulation* **16**, 3143–3421 (2002).
51. Murata, H., Hruz, P. W. & Mueckler, M. Indinavir inhibits the glucose transporter isoform Glut4 at physiologic concentrations. *AIDS* **16**, 859–863 (2002).
52. Hruz, P. W., Yan, Q., Struthers, H. & Jay, P. Y. HIV protease inhibitors that block GLUT4 precipitate acute, decompensated heart failure in a mouse model of dilated cardiomyopathy. *FASEB* **22**, 2161–2167 (2008).
53. Hruz, P. HIV protease inhibitors and insulin resistance: lessons from in vitro, rodent and healthy human volunteer models. *Diabetes* **3**, 660–665 (2009).
54. Germinario, R. J., Colby-Germinario, S. P., Cammalleri, C. & Wainberg, M. A. The long-term effects of anti-retroviral protease inhibitors on sugar transport in L6 cells. *J Endocrinol* **178**, 449–456 (2003).
55. Hertel, J., Struthers, H., Horj, C. & Hruw, P. A structural basis for the acute effects of HIV protease inhibitors on GLUT4 intrinsic activity. *J Biol Chem* **279**, 55147–55152 (2004).
56. Liang, J.-S. et al. HIV protease inhibitors protect apolipoprotein B from degradation by the proteasome: A potential mechanism for protease inhibitor-induced hyperlipidemia. *Nat Med* **7**, 1327–1331 (2001).
57. Parker, R. A. et al. Endoplasmic reticulum stress links dyslipidemia to inhibition of proteasome activity and glucose transport by HIV protease inhibitors. *Mol Pharmacol* **67**, 1909–1919 (2005).
58. Behrens, G. et al. Impaired glucose tolerance, beta cell function and lipid metabolism in HIV patients under treatment with protease inhibitors. *AIDS* **13**, F63–70 (1999).
59. Bastard, J. et al. Association between altered expression of adipogenic factor SREBP1 in lipoatrophic adipose tissue from HIV-1-infected patients and abnormal adipocyte differentiation and insulin resistance. *Lancet* **359**, 1026–1031 (2002).
60. Carr, A. et al. HIV protease inhibitor substitution in patients with lipodystrophy: a randomized, controlled, open-label, multicentre study. *AIDS* **15**, 1811–1822 (2001).
61. Dong, K. et al. Changes in body habitus and serum lipid abnormalities in HIV-positive women on highly active antiretroviral therapy (HAART). *J AIDS* **21**, 107–113 (1999).
62. Gan, S. et al. Altered myocellular and abdominal fat partitioning predict disturbance in insulin action in HIV protease inhibitor-related Lipodystrophy. *Diabetes* **51**, 3163–3169 (2002).
63. Tsiodras, S., Mantzoros, C., Hammer, S. & Samore, M. Effects of protease inhibitors on hyperglycemia, hyperlipidemia, and lipodystrophy: a 5-year cohort study. *Arch Intern Med* **160**, 2050–2056 (2000).
64. Floris-Moore, M. et al. Increased serum lipids are associated with higher CD4 lymphocyte count in HIV-infected women. *HIV Med* **7**, 421–430 (2006).

65. Rudich, A., Ben-Romano, R., Etzion, S. & Bashan, N. Cellular mechanisms of insulin resistance, lipodystrophy and atherosclerosis induced by HIV protease inhibitors. *Acta Physiol Scand* **183**, 75–88 (2005).
66. Behrens, G. M. N. et al. Impaired glucose phosphorylation and transport in skeletal muscle cause insulin resistance in HIV-1 – infected patients with lipodystrophy. *J Clin Invest* **110**, 1319–1327 (2002).
67. Woerle, H. et al. Mechanisms for the deterioration in glucose tolerance associated with HIV protease inhibitor regimens. *Diabetes* **52**, 918–925 (2003).
68. Dube, M. P. Disorders of Glucose Metabolism in Patients Infected with Human Immunodeficiency Virus. *Clin Infect Dis* **31**, 1467–1475 (2000).
69. Walli, R., et. al. Treatment with protease inhibitors associated with peripheral insulin resistance and impaired glucose tolerance in HIV-1-infected patients. *AIDS* **12**, F167–173 (1998).
70. Chance, B., Sies, H. & Boveris, H. Hydroperoxide metabolism in mammalian organs. *Physiol Rev* **59**, 527–605 (1979).
71. Zaera, Â., Cardellach, F., Casademont, J. & Nunes, V. Mitochondrial involvement in antiretroviral therapy- related lipodystrophy. *AIDS* 1643–1651 (2001).
72. Zhang, S. et al. Protease inhibitors used in the treatment of HIV+ induce beta-cell apoptosis via the mitochondrial pathway and compromise insulin secretion. *Am J Physiol Endocrinol Metab* **296**, E925–935 (2009).
73. Lagathu, C. et al. Some HIV antiretrovirals increase oxidative stress and alter chemokine, cytokine or adiponectin production in human adipocytes and macrophages. *Antivir. Ther.* **12**, 489–500 (2007).
74. Chandra, S., Mondal, D. & Agrawal, K. C. HIV-1 protease inhibitor induced oxidative stress suppresses glucose stimulated insulin release: protection with thymoquinone. *Exp Biol Med* **234**, 442–453 (2009).
75. Touzet, O. & Philips, A. Resveratrol protects against protease inhibitor-induced reactive oxygen species production, reticulum stress and lipid raft perturbation. *AIDS* **24**, 1437–1447 (2010).
76. Ben-Romano, R. et al. Nelfinavir induces adipocyte insulin resistance through the induction of oxidative stress: differential protective effect of antioxidant agents. *Antivir. Ther.* **11**, 1051–1060 (2006).
77. Wang, X., Chai, H., Lin, P. H., Yao, Q. & Chen, C. Roles and mechanisms of human immunodeficiency virus protease inhibitor ritonavir and other anti-human immunodeficiency virus drugs in endothelial dysfunction of porcine pulmonary arteries and human pulmonary artery endothelial cells. *Am J Pathol* **174**, 771–781 (2009).
78. Wang, X. et al. Human immunodeficiency virus protease inhibitor Ritonavir inhibits cholesterol efflux from human macrophage-derived foam cells. *Am J Pathol* **171**, 304–314 (2007).
79. Conklin, B. S. et al. HIV protease inhibitor ritonavir decreases endothelium-dependent vasorelaxation and increases superoxide in porcine arteries. *Cardiovasc Res* **63**, 168–175 (2004).

80. Lagathu, C. *et al.* Some HIV antiretrovirals increase oxidative stress and alter chemokine, cytokine or adiponectin production in human adipocytes and macrophages. *Antivir. Ther.* **12**, 489–500 (2007).
81. Deng, W., Baki, L., Yin, J., Zhou, H. & Baumgarten, C. M. HIV protease inhibitors elicit volume-sensitive Cl[−] current in cardiac myocytes via mitochondrial ROS. *J Mol Cell Cardiol* **49**, 746–752 (2010).
82. Chai, H. *et al.* Effects of 5 HIV protease inhibitors on vasomotor function and superoxide anion production in porcine coronary arteries. *J AIDS* **40**, 12–19 (2005).
83. Jiang, B. *et al.* HIV antiretroviral drug combination induces endothelial mitochondrial dysfunction and reactive oxygen species production, but not apoptosis. *Toxicol Appl Pharmacol* **224**, 60–71 (2007).
84. Mondal, D., Pradhan, L., Ali, M. & Agrawal, K. C. HAART drugs induce oxidative stress in human endothelial cells and increase endothelial recruitment of mononuclear cells: exacerbation by inflammatory cytokines and amelioration by antioxidants. *Cardiovasc Toxicol* **4**, 287–302 (2004).
85. Chai, H., Yan, S., Lin, P. & Lumsden, A. B. Curcumin blocks HIV protease inhibitor ritonavir-induced vascular dysfunction in porcine coronary arteries. *J Am Coll Sur* **200**, 820–830 (2005).
86. Chen, Q., Vazquez, E., Moghaddas, S., Hoppel, C. & Lesnefsky, E. Production of reactive oxygen species by mitochondria. *J Biol Chem* **278**, 36027–36031 (2003).
87. St-Pierre, J., Buckingham, J., Roebuck, S. & Brand, M. Topology of superoxide production from different sites in the mitochondrial electron transport chain. *J Biol Chem* **277**, 44784–44790 (2002).
88. Gupte, R. S. *et al.* Upregulation of glucose-6-phosphate dehydrogenase and NAD(P)H oxidase activity increases oxidative stress in failing human heart. *J Card. Fail* **13**, 497–506 (2007).
89. Varela, D., Simon, F., Riveros, A., Jorgensen, F. & Stutzin, A. NAD(P)H oxidase-derived H₂O₂ signals chloride channel activation in cell volume regulation and cell proliferation. *J Biol Chem* **279**, 13301–13304 (2004).
90. Zweier, J. & Talukder, M. The role of oxidants and free radicals in reperfusion injury. *Cardiovasc Res* **70**, 181–190 (2006).
91. Pacher, P., Nivorozhkin, A. & Szabo, C. Therapeutic effects of xanthine oxidase inhibitors: renaissance half a century after the discovery of allopurinol. *Pharmacol Rev* **58**, 87–114 (2006).
92. Van der Vusse, G. J., van Bilsen, M. & Glatz, J. F. Cardiac fatty acid uptake and transport in health and disease. *Cardiovasc Res* **45**, 279–293 (2000).
93. Akki, A., Zhang, M., Murdoch, C., Brewer, A. & Shah, A. NADPH oxidase signaling and cardiac myocyte function. *J Mol Cell Cardiol* **47**, 15–22 (2009).
94. Zorov, D. B., Juhaszova, M. & Sollott, S. J. Mitochondrial ROS-induced ROS release : an update and review. *Biochim Biophys Acta* **1757**, 509–517 (2006).
95. McCord, J. & Fridovich, I. An enzymatic function for erythrocuprein (hemocuprein). *J Biol Chem* **244**, 6049–6055 (1969).

96. Antunes, F., Han, D. & Cadenas, E. Relative contributions of heart mitochondria glutathione peroxidase and catalase to H₂O₂ detoxification in in vivo conditions. *Free Rad Biol Med* **33**, 1260–1267 (2002).
97. Finkel, T. Oxidant signals and oxidative stress. *Curr Opin Cell Biol* **15**, 247–254 (2003).
98. Giordano, F. Oxygen, oxidative stress, hypoxia, and heart failure. *J Clin Invest* **115**, 500–508 (2005).
99. Kurosawa, K., et al. Kinetics of hydrogen peroxide degradation by NADP glutathione system in mitochondria. *J Biochem* **108**, 9–16 (1990).
100. Lambeth, J. NOX enzymes and the biology of reactive oxygen. *Nat Rev Immunol* **4**, 181–189 (2004).
101. Cave, A. et al. NADPH oxidases in cardiovascular health and disease. *Antioxid Redox Signal* **8**, 691–728 (2006).
102. Bedard, K. & Krause, K. The NOX family of ROS-generating NADPH oxidases: physiology and pathophysiology. *Physiol Rev* **87**, 245–313 (2007).
103. Charbit, B., Gayat, E., Voiriot, P., Boccard, F. & Girard, P. Effects of HIV protease inhibitors on cardiac conduction velocity in unselected HIV-infected patients. *Clin Pharmacol Ther.* **90**, 442–448 (2009).
104. Gutteridge, J. Iron promoters of the Fenton reaction and lipid peroxidation can be released from haemoglobin by peroxides. *FEBS Lett.* **201**, 291–295 (1986).
105. Brownlee, M. The pathobiology of diabetic complications: a unifying mechanism. *Diabetes* **54**, 1615–25 (2005).
106. Giacco, F. & Brownlee, M. Oxidative stress and diabetic complications. *Circ. Res.* **107**, 1058–70 (2010).
107. Nishikawa, T. et al. Normalizing mitochondrial superoxide production blocks three pathways of hyperglycaemic damage. *Nature* **404**, 787–90 (2000).
108. Beltramo, E., Berrone, E., Tarallo, S. & Porta, M. Effects of thiamine and benfotiamine on intracellular glucose metabolism and relevance in the prevention of diabetic complications. *Acta Diabetol.* **45**, 131–41 (2008).
109. Katore, R. G. et al. Vitamin B1 analog benfotiamine prevents diabetes-induced diastolic dysfunction and heart failure through Akt/Pim-1-mediated survival pathway. *Circ. Heart Fail.* **3**, 294–305 (2010).
110. Chung, S. S. M. Contribution of Polyol Pathway to Diabetes-Induced Oxidative Stress. *J. Am. Soc. Nephrol.* **14**, 233S–236 (2003).
111. Cheng, H. M., & Gonzalez, R. G. The effect of high glucose and oxidative stress on lens metabolism, aldose reductase, and senile cataractogenesis. *Metabolism* **35**, 10–14 (1986).

112. Morre, D. M., Lenaz, G., & Morre, D. J. Surface oxidase and oxidative stress propagation in aging. *J Exp Biol* **203**, 1513–1521 (2000).
113. Oates, P. J. & Mylari, B. L. Aldose reductase inhibitors: Therapeutic implications for diabetic complications. *Expert Opin Investig Drugs* **8**, 2095–2119 (1999).
114. Gonzalez, A. M., Sochor, M., & McLean, P. The effect of an aldose reductase inhibitor (Sorbitol) on the level of metabolites in lenses of diabetic rats. *Diabetes* **32**, 482–485 (1983).
115. Ng, T. F., et. al. Effects of sorbitol dehydrogenase deficiency on nerve conduction in experimental diabetic mice. *Diabetes* **47**, 961–966 (1998).
116. Lou, M. F., Dickerson Jr, J. E., Garadi, R. & York Jr, B. M. Glutathione depletion in the lens of galactosemic and diabetic rats. *Exp Eye Res.* **46**, 517–530 (1988).
117. Obrosova, I. G., Fathallah, L. & Lang, H. Interaction between Osmotic and Oxidative Stress in Diabetic Precataractous Lens. *Biochem Pharma* **58**, 1945–1954 (1999).
118. Singh, R., Barden, a, Mori, T. & Beilin, L. Advanced glycation end-products: a review. *Diabetologia* **44**, 129–46 (2001).
119. Brownlee, M. Advanced protein glycosylation in diabetes and aging. *Annu Rev Med* **46**, 223–234 (1995).
120. Tanaka, S., et. al. Glycation induces expansion of the molecular packaging of collagen. *J Mol Biol* **203**, 495–505 (1988).
121. Baynes, J. W., & Thorpe, S. R. Role of oxidative stress in diabetic complications: a new perspective on an old paradigm. *Diabetes* **48**, 1–9 (1999).
122. Suzuki, D., et. al. Immunohistochemical evidence for an increased oxidative stress and carbonyl modification of proteins in diabetic glomerular lesions. *J Am Soc Nephrol* **10**, 822–832 (1999).
123. Gkogkolou, P. & Böhm, M. Advanced glycation end products: Key players in skin aging? *Dermatoendocrinol.* **4**, 259–70 (2012).
124. Thornalley, P. J. Pharmacology of methylglyoxal. *Gen Pharmacol* **27**, 565–573 (1996).
125. Thornalley, P. J., et. al. Formation of methylglyoxal - modified proteins in vitro and in vivo and their involvement in AGE-related processes. *Contrib Nephrol* **112**, 24–31 (1995).
126. Thornalley, P. J., Langborg, A., & Minhas, H. S. Formation of glyoxal, methylglyoxal and 3-DG in the glycation of proteins. *Biochem J* **344**, 109–116 (1999).
127. Okado, a *et al.* Induction of apoptotic cell death by methylglyoxal and 3-deoxyglucosone in macrophage-derived cell lines. *Biochem. Biophys. Res. Commun.* **225**, 219–24 (1996).
128. Fukunaga, M. *et al.* Methylglyoxal induces apoptosis through activation of p38 MAPK in rat Schwann cells. *Biochem. Biophys. Res. Commun.* **320**, 689–95 (2004).

129. Kikuchi, S. *et al.* Neurotoxicity of methylglyoxal and 3-deoxyglucosone on cultured cortical neurons: synergism between glycation and oxidative stress, possibly involved in neurodegenerative diseases. *J. Neurosci. Res.* **57**, 280–9 (1999).
130. Liu, B.-F. *et al.* Methylglyoxal induces apoptosis through activation of p38 mitogen-activated protein kinase in rat mesangial cells. *Kidney Int.* **63**, 947–57 (2003).
131. Zarubin, T. & Han, J. Activation and signaling of the p38 MAP kinase pathway. *Cell Res.* **15**, 11–8 (2005).
132. Yamagishi, S. & Imaizumi, T. Diabetic vascular complications: pathophysiology, biochemical basis and potential therapeutic strategy. *Curr. Pharm. Des.* **11**, 2279–99 (2005).
133. Bucala, R., Tracey, K. J. & Cerami, a. Advanced glycosylation products quench nitric oxide and mediate defective endothelium-dependent vasodilatation in experimental diabetes. *J. Clin. Invest.* **87**, 432–8 (1991).
134. Basta, G., Schmidt, A. M. & De Caterina, R. Advanced glycation end products and vascular inflammation: implications for accelerated atherosclerosis in diabetes. *Cardiovasc. Res.* **63**, 582–92 (2004).
135. Chiarelli, F., *et. al.* Advanced glycation end-products in children and adolescents with diabetes mellitus: relation to glycaemic control and early microvascular complications. *J Pediatr* **34**, 486–491 (1999).
136. Lee, A. T., & Cerami, A. Role of glycation in aging. *Ann NY Acad Sci* **663**, 63–70 (1992).
137. Bucala, R., & Cerami, A. Advanced glycation: chemistry, biology and implications for diabetes and aging. *Adv Pharmacol* **23**, 1–34 (1992).
138. Raj, D. S., *et. al.* AGE: a nephrologist's perspective. *Am J Kidney Dis* **35**, 365–380 (2000).
139. Ceriello, A. Hyperglycaemia: the bridge between non-enzymatic glycation and oxidative stress in the pathogenesis of diabetic complications. *Diabetes Nutr Metab* **12**, 42–46 (1999).
140. Scivittaro, V., Ganz, M. B., & Weiss, M. F. AGE induce oxidative stress and activate protein kinase C-beta (II) in neonatal mesangial cells. *Am J Physiol* **278**, F676–683 (2000).
141. McCance, D. R., *et. al.* Maillard reaction products and their relation to complications in insulin dependant diabetes mellitus. *J Clin Invest* **91**, 2470–2478 (1993).
142. Boel, E., *et. al.* Diabetic late complications: will aldose reductase inhibitors or inhibitors of advanced glycosylation end-product formation hold promise? *J Diabetes Complicat.* **9**, 104–129 (1995).
143. Munch, G., Thome, J., Foley, P., Schinzel, R. & Riederer, P. Advanced glycation endproducts in ageing and Alzheimer's disease. *Brain Res. Rev.* **23**, 134–143 (1997).
144. Schmidt, A. M., *et. al.* Activation of receptor for advanced glycation end products: a mechanism for chronic vascular dysfunction in diabetic vasculopathy and atherosclerosis. *Circ Res* **84**, 489–497 (1999).

145. Knecht, K. J., Feather, M. S., & Baynes, J. W. Detection of 3-deoxyfructose and 3-deoxyglucosone in human urine and plasma: evidence for intermediate stages of the Maillard reaction in vivo. *Arch Biochem Biophys* **294**, 130–137 (1992).
146. Schmidt, A. M., et. al. Cellular receptors for advanced glycation end products: implications for induction of oxidant stress and cellular dysfunction in the pathogenesis of vascular lesions. *Arter. Thromb.* **14**, 1521–1528 (1994).
147. Schmidt, A. M., et. al. Receptor for advanced glycation end products (AGEs) has a central role in vessel wall interactions and gene activation in response to circulating AGE proteins. *Proc Natl Acad Sci USA* **91**, 8807–8811 (1994).
148. Fu, M. X., et. al. Glycation, glycoxidation, and cross-linking of collagen by glucose: kinetics, mechanisms, and inhibition of late stages of the Maillard reaction. *Diabetes* **43**, 676–683 (1994).
149. Newton, A. C. Protein Kinase C : Structure , Function , and Regulation *. *J Biol Chem* **270**, 28495–28498 (1995).
150. Mellor, H. & Parker, P. J. The extended protein kinase C superfamily. *Biochem. J.* **332** (Pt 2, 281–92 (1998).
151. Asaoka, Y., et. al. Protein kinase C, calcium and phospholipid degradation. *Trends Biochem Sci* **17**, 414–417 (1992).
152. Nishizuka, Y. Intracellular signaling by hydrolysis of phospholipids and activation of protein kinase C. *Science* **258**, 607–14 (1992).
153. Nishizuka, Y. Protein kinase C and lipid signaling for sustained cellular responses. *FASEB* **9**, 484–496 (1995).
154. Thomas, R. No Title. (2011). at <<http://www.biotek.uio.no/english/research/groups/leitges-group/background-information/>>
155. Kennelly, P. J. & Krebs, E. G. Consensus sequences as substrate specificity determinants for protein kinases and protein phosphatases. *J. Biol. Chem.* **266**, 15555–8 (1991).
156. Eller, M., et. al. Substrate Specificity of Protein Kinase C Studied with Peptides Containing D-Amino Acid Residues. *J Biochem* **114**, 177–180 (1993).
157. O'Brian, C., & Ward, N. E. Stimulation of the ATPase activity of rat brain protein kinase C by phospho acceptor substrates of the enzyme. *Biochemistry* **30**, 2549–2554 (1991).
158. Nishizuka, Y. Studies and perspectives of protein kinase C. *Science.* **233**, 305–312 (1986).
159. Dekker, L. V., & Parker, P. J. Protein kinase C--a question of specificity. *Trends Biochem Sci* **19**, 73–77 (1994).
160. Inoguchi, T. et al. Preferential elevation of protein kinase C isoform beta II and diacylglycerol levels in the aorta and heart of diabetic rats : Differential reversibility to glycemic control by islet cell transplantation. **89**, 11059–11063 (1992).

161. Inoguchi, T., et. al. Insulin's effect on protein kinase C and diacylglycerol induced by diabetes and glucose in vascular tissues. *Am J Physiol* **267**, E369–379 (1994).
162. Shiba, T., et. al. Correlation of diacylglycerol level and protein kinase C activity in rat retina to retinal circulation. *Am J Physiol* **265**, E783–793 (1993).
163. Xia, P., et. al. Characterization of the mechanism for the chronic activation of diacylglycerol-protein kinase C pathway in diabetes and hypergalactosemia. *Diabetes* **43**, 1122–1129 (1994).
164. Craven, P. A., & DeRubertis, F. R. Protein kinase C is activated in glomeruli from streptozotocin diabetic rats. Possible mediation by glucose. *J Clin Invest* **83**, 1667–1675 (1989).
165. Wolf, B. a *et al.* Diacylglycerol accumulation and microvascular abnormalities induced by elevated glucose levels. *J. Clin. Invest.* **87**, 31–8 (1991).
166. Studor, P.K., Craven, P. A., & DeRubertis, F. R. Role of protein kinase C in the mediation of increased fibronectin accumulation by mesangial cells grown in high-glucose medium. *Diabetes* **42**, 118 (1993).
167. Tesfamariam, B., Brown, M. L., & Cohen, R. A. Elevated glucose impairs endothelium-dependent relaxation by activating protein kinase C. *J Clin Invest* **87**, 1643–1648 (1991).
168. Ishii, H., et. al. Amelioration of vascular dysfunctions in diabetic rats by an oral PKC beta inhibitor. *Science (80-.).* **272**, 728 (1996).
169. Kuroki, T., et. al. High glucose induces alteration of gap junction permeability and phosphorylation of connexin-43 in cultured aortic smooth muscle cells. *Diabetes* **47**, 931–936 (1998).
170. Koya, D., et. al. Amelioration of accelerated diabetic mesangial expansion by treatment with a PKC β inhibitor in diabetic db/db mice, a rodent model for type 2 diabetes. *FASEB* **14**, 439–447 (2000).
171. Lee, T., Saltsman, K. A., Ohashi, H. & King, G. L. Activation of protein kinase C by elevation of glucose concentration: Proposal for a mechanism in the development of diabetic vascular complications. *Proc. Natl. Acad. Sci. U. S. A.* **86**, 5141–5145 (1989).
172. Inoguchi, T. Protein Kinase C-Dependent Increase in Reactive Oxygen Species (ROS) Production in Vascular Tissues of Diabetes: Role of Vascular NAD(P)H Oxidase. *J. Am. Soc. Nephrol.* **14**, 227S–232 (2003).
173. Marshall, S., Garvey, W. T., & Traxinger, R. R. New insights into the metabolic regulation of insulin action and insulin resistance: role of glucose and amino acids. *FASEB J* **5**, 3031–3036 (1991).
174. Marshall, S., Bacote, V. & Traxinger, R. R. Discovery of a Metabolic Pathway Mediating Glucose-induced Desensitization of the Glucose Transport System. Role of hexosamine biosynthesis in the induction of insulin resistance. *J Biol Chem* **266**, 4706–4712 (1991).
175. McKnight, G. L. *et al.* Molecular cloning, cDNA sequence, and bacterial expression of human glutamine: fructose-6-phosphate amidotransferase. *J Biol Chem* **267**, 25208–25212 (1992).

176. Sayeski, P. P. & Kudlow, J. E. Glucose metabolism to glucosamine is necessary for glucose stimulation of transforming growth factor- α gene transcription. *J Biol Chem* **271**, 15237–15243 (1996).
177. Zhou, J. *et al.* Regulation of glutamine:fructose-6-phosphate amidotransferase by cAMP-dependant protein kinase. *Diabetes* **47**, 1836–1840 (1998).
178. Hawkins, M., *et al.* Role of the glucosamine pathway in fat-induced insulin resistance. *J Clin Invest* **99**, 2173–2182 (1997).
179. Schleicher, E. D., & Weigert, C. Role of the hexosamine biosynthetic pathway in diabetic nephropathy. *Kidney Int.* **58**, S13–18 (2000).
180. Hart, G. W. Dynamic O-linked glycosylation of nuclear and cytoskeletal proteins. *Annu Rev Biochem* **66**, 315–335 (1997).
181. Zachara, N. E. & Hart, G. W. Cell signalling, the essential role of OGlcNAc! *Biochim Biophys Acta* **1761**, 599–617 (2006).
182. Jochmann, R. *et al.* O-linked N-acetylglucosaminylation of Sp1 inhibits the human immunodeficiency virus type 1 promoter. *J. Virol.* **83**, 3704–18 (2009).
183. Iyer, S. P. & Hart, G. W. Dynamic nuclear and cytoplasmic glycosylation: enzymes of O-GlcNAc cycling. *Biochemistry* **42**, 2493–2499 (2003).
184. Haltiwanger, R. S., Grove, K. & Philipsberg, G. A. Modulation of O-linked N-acetylglucosamine levels on nuclear and cytoplasmic proteins in vivo using the peptide O-GlcNAc-beta-N-acetylglucosaminidase inhibitor O-[2-acetamido-2-deoxy-D-glucopyranosylidene]-amino-N-phenylcarbamate. *J Biol Chem* **273**, 3611–3617 (1998).
185. Kang, H. T., *et al.* Down-regulation of Sp1 activity through modulation of O-glycosylation by treatment with a low glucose mimetic 2-deoxyglucose. *J Biol Chem* **278**, 51223–51231 (2003).
186. Roos, M. D., *et al.* Streptozotocin, an analog of N-acetylglucosamine, blocks the removal of O-GlcNAc from intracellular proteins. *Proc Assoc Am Physicians* **110**, 422–432 (1998).
187. Du, X. . *et al.* Hyperglycemia inhibits endothelial nitric oxide synthase activity by posttranslational modification at the Akt site. *J Clin Invest* **108**, 1341–1348 (2001).
188. Federici, M. *et al.* Insulin-dependent activation of endothelial nitric oxide synthase is impaired by O-linked glycosylation modification of signaling proteins in human coronary endothelial cells. *Circulation* **106**, 466–472 (2002).
189. Parker, G. ., Lund, K. ., Taylor, R. . & McClain, D. . Insulin resistance of glycogen synthase mediated by O-linked N-acetylglucosamine. *J Biol Chem* **278**, 10022–10027 (2003).
190. Han, I., Roos, M. . & Kudlow, J. . Interaction of the transcription factor Sp1 with the nuclear pore protein p62 requires the C-terminal domain of p62. *J Cell Biochem* **68**, 50–61 (1998).
191. Roos, M. ., Su, K., Baker, J. . & Kudlow, J. . O-glycosylation of an Sp1-derived peptide blocks known Sp1 protein interactions. *Mol Cell Biol* **17**, 6472–6480 (1997).

192. Yang, X. *et al.* O-linkage of N-acetylglucosamine to Sp1 activation domain inhibits its transcriptional capability. *Proc Natl Acad Sci USA* **98**, 6611–6616 (2001).
193. Gao, Y., Miyazaki, J. & Hart, G. . The transcription factor PDX-1 is post-translationally modified by O-linked N-acetylglucosamine and this modification is correlated with its DNA binding activity and insulin secretion in min6 beta-cells. *Arch Biochem Biophys* **415**, 155–163 (2003).
194. Juang, Y. ., Solomou, E. ., Rellahan, B. & Tsokos, G. . Phosphorylation and O-linked glycosylation of Elf-1 leads to its translocation to the nucleus and binding to the promoter of the TCR zeta-chain. *J Immunol* **168**, 2865–2871 (2002).
195. Bachmann, M., Pfeifer, K., Schroder, H. . & Muller, W. . The La antigen shuttles between the nucleus and the cytoplasm in CV-1 cells. *Mol Cell Biochem* **85**, 103–114 (1989).
196. Duverger, E., Roche, A. . & Monsigny, M. N-acetylglucosamine-dependent nuclear import of neoglycoproteins. *Glycobiology* **6**, 381–386 (1996).
197. Duverger, E., Carpentier, V., Roche, A. . & Monsigny, M. Sugar-dependent nuclear import of glycoconjugates from the cytosol. *Exp Cell Res* **207**, 197–201 (1993).
198. Duverger, E., Pellerin-Mendes, C., Mayer, R., Roche, A. . & Monsigny, M. Nuclear import of glycoconjugates is distinct from the classical NLS pathway. *J Cell Sci* **108**, 1325–1332 (1995).
199. Datta, B., Ray, M. ., Chakrabarti, D., Wylie, D. . & Gupta, N. . Glycosylation of eukaryotic peptide chain initiation factor 2 (eIF-2)-associated 67-kDa polypeptide (p67) and its possible role in the inhibition of eIF-2 kinase-catalyzed phosphorylation of the eIF-2 alpha-subunit. *J Biol Chem* **264**, 20620–20624 (1989).
200. Ray, M. . *et al.* The eukaryotic initiation factor 2-associated 67-kDa polypeptide (p67) plays a critical role in regulation of protein synthesis initiation in animal cells. *Proc Natl Acad Sci USA* **89**, 539–543 (1992).
201. Han, I. & Kudlow, J. . Reduced O-glycosylation of Sp1 is associated with increased proteasome susceptibility. *Mol Cell Biol* **17**, 2550–2558 (1997).
202. Cheng, X., Cole, R. ., Zaia, J. & Hart, G. . Alternative O-glycosylation/O-phosphorylation of the murine estrogen receptor beta. *Biochemistry* **39**, 11609–11620 (2000).
203. Du, X. *et al.* Hyperglycemic-induced mitochondrial superoxide overproduction activates the hexosamine pathway and induces plasminogen activator inhibitor-1 expression by increasing Sp1 glycosylation. *PNAS* **97**, 12222–12226 (2000).
204. Chen, Y. *et al.* Sp1 Sites Mediate Activation of the Plasminogen Activator Inhibitor-1 Promoter by Glucose in Vascular Smooth Muscle Cells. *J. Biol. Chem.* **273**, 8225–8231 (1998).
205. Popov, S. G. *et al.* Lethal toxin of Bacillus anthracis causes apoptosis of macrophages. *Biochem. Biophys. Res. Commun.* **293**, 349–55 (2002).
206. Distelhorst, C. W. Recent insights into the mechanism of glucocorticosteroid-induced apoptosis. *Cell Death Differ.* **9**, 6–19 (2002).

207. Rajah, R., Valentinis, B. & Pinchas, C. Insulin-like Growth Factor (IGF)-binding Protein-3 Induces Apoptosis and Mediates the Effects of Transforming Growth Factor-beta 1 on Programmed Cell Death through a p53- and IGF-independent Mechanism. *J. Biol. Chem.* **272**, 12181–12188 (1997).
208. Brüne, B. Nitric oxide: NO apoptosis or turning it ON? *Cell Death Differ.* **10**, 864–9 (2003).
209. Ross, M. E. & Caligiuri, M. a. Cytokine-induced apoptosis of human natural killer cells identifies a novel mechanism to regulate the innate immune response. *Blood* **89**, 910–8 (1997).
210. Takahisa, F., Kong-Woo, Y., Taiji, K. & Kazuo, Y. Heat-induced Apoptosis in Human Glioblastoma Cell Line A172. *Neurosurgery* **42**, 843–849 (1998).
211. Verheij, M. & Bartelink, H. Radiation-induced apoptosis. *Cell Tissue Res.* **301**, 133–42 (2000).
212. Chern, C. L., Huang, R. F., Chen, Y. H., Cheng, J. T. & Liu, T. Z. Folate deficiency-induced oxidative stress and apoptosis are mediated via homocysteine-dependent overproduction of hydrogen peroxide and enhanced activation of NF-kappaB in human Hep G2 cells. *Biomed. Pharmacother.* **55**, 434–42 (2001).
213. Banki, K., Hutter, E., Gonochoroff, N. J. & Perl, A. Molecular Ordering in HIV-induced Apoptosis. Oxidative stress, activation of caspases, and cell survival are regulated by transaldolase. *J. Biol. Chem.* **273**, 11944–11953 (1998).
214. Long, X. *et al.* P53 and the Hypoxia-Induced Apoptosis of Cultured Neonatal Rat Cardiac Myocytes. *J. Clin. Invest.* **99**, 2635–43 (1997).
215. Mattson, M. P. & Chan, S. L. Calcium orchestrates apoptosis. *Nat. Cell Biol.* **5**, 1041–3 (2003).
216. Boehning, D. *et al.* Cytochrome c binds to inositol (1,4,5) trisphosphate receptors, amplifying calcium-dependent apoptosis. *Nat. Cell Biol.* **5**, 1051–61 (2003).
217. Glazner, G. W., Camandola, S., Geiger, J. D. & Mattson, M. P. Endoplasmic reticulum D-myo-inositol 1,4,5-trisphosphate-sensitive stores regulate nuclear factor-kappaB binding activity in a calcium-independent manner. *J. Biol. Chem.* **276**, 22461–7 (2001).
218. Solary, E., Dubrez, L. & Eymen, B. The role of apoptosis in the pathogenesis and treatment of diseases. *Eur. Respir. J.* **9**, 1293–1305 (1996).
219. Terai, C., Kornbluth, R. S., Pauza, C. D., Richman, D. D. & Carson, D. a. Apoptosis as a mechanism of cell death in cultured T lymphoblasts acutely infected with HIV-1. *J. Clin. Invest.* **87**, 1710–5 (1991).
220. Banda, B. N. K. *et al.* Crosslinking CD4 by Human Immunodeficiency Virus gp120 Primes T Cells for Activation-induced Apoptosis. *J Exp Med* **176**, 1099–1106 (1992).
221. Kuida, K., *et al.* Decreased apoptosis in the brain and premature lethality in CPP32-deficient mice. *Nature* **384**, 368–372 (1996).
222. Woo, M., *et al.* Essential contribution of caspase-3/CPP32 to apoptosis and its associated nuclear changes. *Genes Dev* **12**, 806–819 (1998).

223. Janicke, R. U., et. al. Caspase-3 is required for DNA fragmentation and morphological changes associated with apoptosis. *J Biol Chem* **273**, 9357–9360 (1998).
224. Hirata, H., et. al. Caspases are activated in a branched protease cascade and control distinct processes in Fas-induced apoptosis. *J Exp Med* **187**, 587–600 (1998).
225. Nicholson, D. W. & Thornberry, A. Caspases: killer proteases. *Science* (80-.). **22**, 299–306 (1997).
226. Cryns, V. & Yuan, J. Proteases to die for. *Genes Dev* **12**, 1551–1570 (1998).
227. Sloand, E.M., et. al. Human immunodeficiency virus type 1 protease inhibitor modulates activation of peripheral blood CD4(+) T cells and decreases their susceptibility to apoptosis in vitro and in vivo. *Blood* **76**, 5966–5973 (1999).
228. Weichold, F. F., et. al. HIV-1 protease inhibitor ritonavir modulates susceptibility to apoptosis of uninfected T cells. *J Hum Virol* **2**, 261–269 (1999).
229. Horvitz, H. R. Genetic control of programmed cell death in the nematode *Caenorhabditis elegans*. *Cancer Res* **59**, S1701–1706 (1999).
230. Vaux, D. L., Weissman, I. L. & Kim, S. K. Prevention of programmed cell death in *Caenorhabditis elegans* by human BCL-2. *Science* (80-.). **258**, 1955–1957 (1992).
231. Yuan, J., et. al. The *C. elegans* cell death gene *ced-3* encodes a protein similar to mammalian interleukin-1B-converting enzyme. *Cell* **75**, 641–652 (1993).
232. Cory, S. & Adams, J. M. The Bcl2 family: regulators of the cellular life-or-death switch. *Nat. Rev. Cancer* **2**, 647–56 (2002).
233. Veis, D. J., et. al. Bcl-2 deficient mice demonstrate fulminant lymphoid apoptosis, polycystic kidneys, and hypopigmented hair. *Cell* **75**, 229–240 (1993).
234. Gross, A., McDonnell, J. M. & Korsmeyer, S. J. Bcl-2 family members and the mitochondria in apoptosis. *Genes Dev* **13**, 1899–1911 (1999).
235. Martinou, J.-C. & Green, D. R. Breaking the mitochondrial barrier. *Nat. Rev Mol Cell Biol* **2**, 63–67 (2001).
236. Mikhailov, V. *et al.* Bcl-2 prevents Bax oligomerization in the mitochondrial outer membrane. *J. Biol. Chem.* **276**, 18361–74 (2001).
237. Datta, S. R., et. al. 14-3-3 proteins and survival kinases cooperate to inactivate BAD by BH3 domain phosphorylation. *Mol Cell* **6**, 41–51 (2000).
238. Lizcano, J. M., Morrice, N. & Cohen, P. Regulation of BAD by cAMP-dependent protein kinase is mediated via phosphorylation of a novel site, Ser155. *Biochem J* **349**, 547–557 (2000).
239. Virdee, K., Parone, P. A. & Tolkovsky, A. M. Phosphorylation of the pro-apoptotic protein BAD on serine 155, a novel site, contributes to cell survival. *Curr Biol* **10**, R883 (2000).
240. Strack, P. R., et. al. Apoptosis mediated by HIV protease is preceded by cleavage of Bcl-2. *Proc Natl Acad Sci USA* **93**, 9571–9576 (1996).

241. Matarrese, P., et. al. Mitochondrial membrane hyperpolarization hijacks activated T lymphocytes toward the apoptotic-prone phenotype: homeostatic mechanisms of HIV protease inhibitors. *J Immunol* **170**, 6006–6015 (2003).

Chapter 2

**The effects of protease inhibitor (Lopinavir/Ritonavir) treatment
on *in vitro* reactive oxygen species levels, programmed cell
death and NOGPs**

Introduction

As earlier discussed in Chapter 1 of this thesis, HIV/AIDS infection targets the immune system of affected individuals with downstream molecular effects such as excessively high ROS levels. Due to the sensitivity of mitochondrial DNA to increases in ROS, mitochondrial dysfunction may arise leading to the development of a plethora of adverse conditions, e.g. T2DM, cancer¹ and CVD including atherosclerosis^{2,3}. HAART and specifically PIs can also induce ROS and this is supported by a number of studies utilizing human-⁴, animal-⁵⁻⁸, and cell-based⁹⁻¹³ models. However, not much is known about the effects of PIs on the heart and we therefore propose higher myocardial ROS levels - *in vitro*.

Increased ROS is also linked to a rise in cell death. For example, Pierce *et al.*¹⁴ found that increases in H₂O₂ induced apoptosis in blastocysts. Similarly Watson *et al.*¹⁵ found that in neutrophils higher Fas protein levels result in increased apoptosis, which can be inhibited by a rise in intracellular GSH. Ironically the mitochondrion is also involved in the induction of apoptosis via its release of cytochrome c in response to death signals¹⁶. Thus the mitochondrion is implicated in both the cause and effect of cell death.

However, PI treatment may inhibit apoptosis. For example, since caspase 3 is a cysteine protease it would be inhibited by PIs resulting in a decrease in cell death^{17,18}. No interrelation between PIs and the cellular levels of anti-apoptotic markers has been established¹⁹. Apoptosis plays a vital role in the maintenance of cell integrity and irregularities in the process may result in various disease pathologies e.g. cancer²⁰ and the

proliferation of HIV/AIDS^{21,22}.

For the first part of this study, apoptotic markers investigated include: 1) Caspase 3, a pro-apoptotic marker responsible for the cleavage of key structural components in cells in addition to disabling vital homeostatic and repair processes²³, 2) Bcl-2, an anti-apoptotic marker involved in the inhibition of cell death via interactions with the mitochondrial membrane, ER and nuclear envelope²⁴, 3) Bax, which forms part of the Bcl-2 family but induces apoptosis via integration into the mitochondrial membrane²⁵, and 4) pBad, the phosphorylated and thus deactivated form of BAD. BAD binds to and inhibits Bcl-2 thereby allowing apoptosis to occur²⁶⁻²⁸. We therefore propose an increase in PI-induced ROS generation and cell death in rat-derived cardiomyoblasts.

The second part of this study attempted to gain greater insights into mechanisms of PI-induced elevation of ROS levels. Since this remains unclear, we here proposed increased NOGP flux as a potential mechanism. The four main pathways implicated in microvascular and macrovascular complications arising from PI-induced hyperglycemia and ROS production are the polyol pathway, AGE pathway, PKC pathway and HBP pathway. For the purpose of this study we investigated the role of PIs in the induction of the NOGPs in rat-derived cardiomyoblasts.

Materials and Methods

Cell culture

Rat-derived cardiomyoblasts (H9c2 cell line, ECACC No. 8809294) were cultured in T25 flasks at 37°C in 5% CO₂ in Dulbecco's Modified Eagle's Medium (DMEM) containing GlutaMAX™, 1 mM (low) glucose (Invitrogen, Carlsbad CA); and supplemented with 10% FBS and 1% penicillin/streptomycin solution (Invitrogen, Carlsbad CA). Typically, cells with a passage number of 12-14 were used for experiments. Cells were cultured at a seeding density of approximately 300 000. A n=4 was used for all experiments.

Evaluation of ROS production

Cells were allowed to reach 70-80% confluency before being subjected to PI treatment, specifically Lopinavir/Ritonavir (Kaletra™, Abbot Laboratories, Abbot Park II), for a period of 24 hours. PIs were administered by resuspending crushed Lopinavir/Ritonavir tablets in DMSO. An initial stock solution of 20 mg/mL was made up, and diluted in 4 mL DMEM per flask to achieve the final concentrations as indicated in Figure 1. Cells receiving no treatment were used as a control, whereas cells receiving only 48 µL (0.012% v/v) DMSO were employed to ascertain the effect of the vehicle.

At the end of the treatment period, cells were harvested via trypsinization and the subsequent pellets were collected and treated with MitoSOX™ Red mitochondrial superoxide indicator dye (1:500; Invitrogen, Carlsbad CA) for 10 min at 37°C. MitoSOX™ Red mitochondrial superoxide indicator dye is a fluorogenic dye which is able to permeate live cells, specifically targeting mitochondria. Upon entering the mitochondria, MitoSOX™ Red reagent is rapidly oxidized by superoxide and exhibits red fluorescence as a result of the oxidation product binding to nucleic acids. The

oxidation of MitoSOX™ Red reagent is specific to superoxide and not to any other ROS- or RNS- (reactive nitrogen species) generating systems²⁹.

Cells were then centrifuged ($5\,000 \times g$, 3 min) and pellets washed and resuspended in with warm PBS. Hereafter the amount of mitochondrial ROS generated was assessed via flow cytometry (BD Bioscience FACS Aria™, Becton Dickinson, San Jose CA), performed at the Central Analytical Facility (CAF) at Stellenbosch University.

A dose response curve was set up to establish optimal dosage of PI required. Cell debris was gated out for analysis. Data were normalized to the control to eliminate the binding of MitoSOX™ to nuclear DNA following oxidation from affecting the results. Ultimately the Lopinavir/Ritonavir dosage of 240 µg/mL was selected. Previous studies on cardiomyocytes by Deng *et al.*³¹ used 9 432 µg/µL of Lopinavir/Ritonavir for 15 minutes. Here the concentration of PI is much higher, however, the treatment time is much less.

Western blotting analysis

Rat-derived cardiomyoblasts (H9c2) were cultured as mentioned previously. A PI concentration of 240 µg/mL was administered to the treatment group for a period of 24 hours. Thereafter, cells were harvested and sonicated for 7 seconds in 1 mL radioimmunoprecipitation assay (RIPA) buffer (50 mM Tris-HCl pH 7.4, 150 mM NaCl, 1% Triton x-100, 1% sodium deoxycholate, 0.1% SDS, 1 mM EDTA) and centrifuged twice at $7\,500 \times g$ for 10 minutes. The resultant supernatant was collected as the protein fraction. Protein concentration was determined by employing the Bradford technique, with BSA as the protein standard.

Samples for Western blotting were prepared by addition of a Laemmli sample buffer containing β -mercaptoethanol to a final protein concentration of 20 μ g. Samples were boiled at 95°C for 5 minutes to ensure denaturation of proteins into a linear formation, capable of migrating through the SDS-PAGE gel. Briefly, prepared samples were then loaded in commercially available 10-well precast Mini-PROTEAN® TGX Stain-Free™ polyacrylamide gels (Bio-Rad, Hercules CA) and subjected to electrophoresis in a 1× running buffer containing 25 mM Tris, 192 mM glycine, 0.1% SDS, and at pH 8.3 (Bio-Rad, Hercules CA). 4 μ l of the protein marker pEqGOLD (PEQLAB Ltd. Sarisbury Green) was loaded as an indicator of protein migration and protein size.

Gels were electrophoresed at 250 V until adequate separation of proteins was achieved. Hereafter transfer of proteins from the gel to the membrane was performed by the employment of commercially available transfer packs in conjunction with the Trans-Blot® Turbo™ Transfer system (Bio-Rad, Hercules CA). The system makes use of semi-dry transfer, ensuring the migration of separated proteins from the gel to the pre-wet polyvinylidene fluoride (PVDF) membrane contained in the transfer pack, in 7 minutes.

The membrane was then subjected to various washing steps in Tris-buffered saline solution containing Tween-20 (2 L TBS-T: 20 mM Tris-HCl, 500 mM NaCl, 2 mL Tween-20). Blocking for the primary antibody was performed for using 5% fat-free milk solution (5 g fat-free dry milk powder dissolved in 100 mL TBS-T solution). The membrane was incubated in primary antibody (1:1000) at 4°C, overnight (Table 1). Incubation in secondary antibody, (goat-anti-rabbit IgG-HRP, Santa Cruz Biotechnologies, CA), at 1:4000 concentration, was performed at room temperature for 1

hour. Visualization of the membrane was performed with enhanced chemiluminescence (ECL).

Table 1: Antibody usage for Western blotting analysis

	Primary antibody	Supplier
Cell Death		
Bcl2	α -rabbit Bcl2	Santa Cruz Biotechnologies, CA
Caspase3	α -rabbit Caspase3	Cell Signaling Technology, MA
pBad	α -rabbit pBad	Santa Cruz Biotechnologies, CA
β-actin	α -rabbit β -actin	Santa Cruz Biotechnologies, CA
Hexosamine biosynthetic pathway		
O-GlcNAc	α -rabbit O-GlcNAc	Cell Signaling Technology, MA

Protein expression was determined by the adjusted percentage volume, (intensity units of pixels of band \times mm²), after background subtraction (Quantity One Software v4.6.9, BioRad, Hercules CA), and normalized to β -actin to correct for loading variations. The adjusted volume for the control group was represented as 100%, and corresponding values for vehicle and treatment groups were expressed as a percentage of the average of the control. This method was performed for each experiment separately before all values were combined in the statistical program. A n=4 was used for each experimental group.

Hexosamine biosynthetic pathway

Western blotting analysis (as described above) was employed to determine total O-GlcNAc expression as a marker for HBP activation.

Advanced glycation end product (AGE) pathway

Methylglyoxal (MG) concentrations were measured by means of a commercial kit (OxiSelect™ MG ELISA Kit; Cell Biolabs, San Diego CA) to assess AGE pathway

activation. MG derivatives are formed via the Maillard reaction - products of this reaction are referred to as AGEs. MG levels were calculated from the standard curve (generated by plotting the absorbance values of standards against the protein concentration and employing the $y=mx+c$ equation) and are expressed as nmol per μg protein.

Protein kinase C (PKC) pathway

The PKC assay was carried out using an ELISA-based commercially available kit (Enzo Life Sciences, Farmingdale NY) and protocol was followed as detailed in the kits instruction manual. PKC activity was determined from the standard curve (generated by plotting the absorbance values of standards against the protein concentration and employing the $y=mx+c$ equation) and expressed per volume of lysate per minute.

Polyol pathway

D-sorbitol levels were measured as detailed in the instructions of a commercially obtained kit (BioVision K 631-100, Mountain View CA). A standard curve was generated by plotting the absorbance values against concentration of protein standards and employing the $y=mx+c$ equation. We then calculated the sorbitol concentration (C) of samples by using the sample amount (nmol) from the standard curve (S_a), sample volume (μL) used (S_v) and the dilution factor (D); $C=S_a/S_v*D$.

Statistical analysis

Statistical analysis was performed by one-way ANOVA and the Bonferroni *post-hoc* test was used to determine differences between groups (GraphPad Prism v5, San Diego CA). Data are presented as mean \pm SEM, and values considered significant when $p<0.05$.

Results

A significant increase in mitochondrial ROS was observed in cells treated with 240 $\mu\text{g/mL}$ PI (Figure 1). This dosage was thus employed in all subsequent cell culture experiments to assess the effects on NOGPs and cell death.

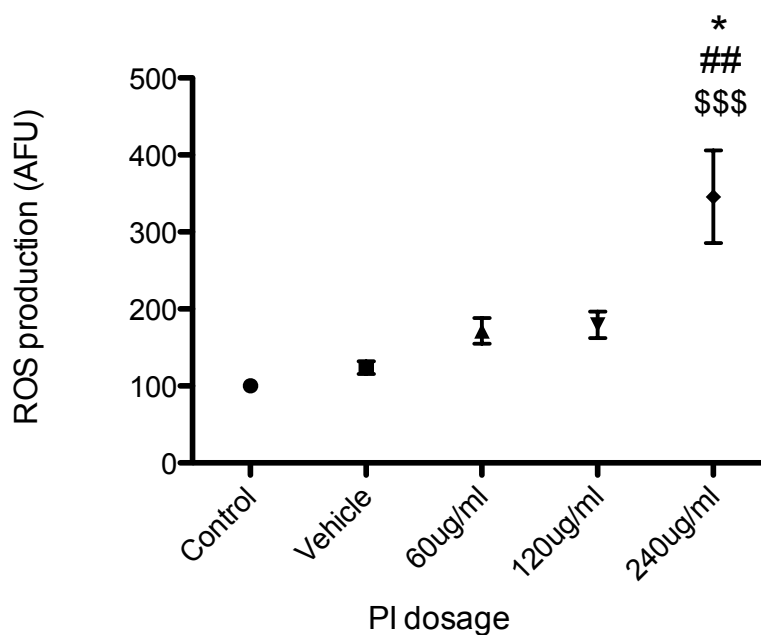


Figure 1: Dose response curve to determine optimal PI dosage. Mitochondrial ROS production in arbitrary fluorescent units (AFU) was plotted against various dosages of Lopinavir/Ritonavir. $\ast = p < 0.05$ vs. 120 $\mu\text{g/mL}$, $\#\# = p < 0.01$ vs. 60 $\mu\text{g/mL}$, $\$\$\$ = p < 0.001$ vs. Control and Vehicle.

Because of the significant PI-induced upregulation in mitochondrial ROS observed in rat-derived cardiomyoblasts, we proposed a related increase in apoptosis. Here cells were subjected to PI treatment at the chosen dose and cell death markers were evaluated. However, no significant changes were observed for any of the apoptotic markers investigated (Figure 2).

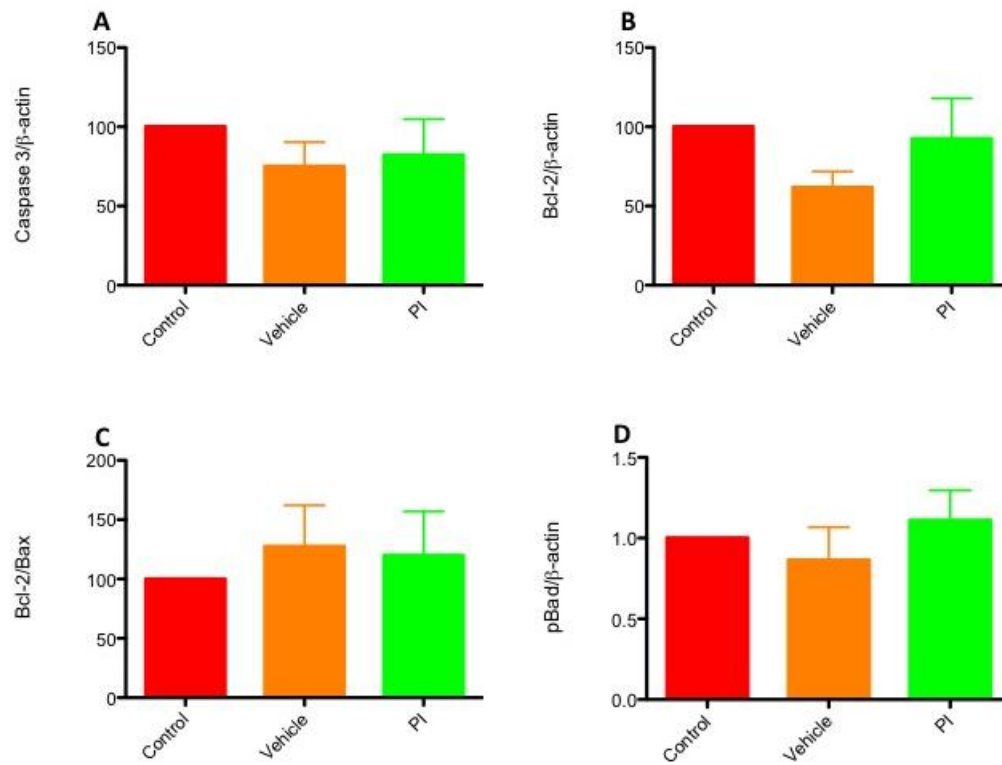


Figure 2. Apoptosis in rat-derived cardiomyoblasts in response to 24 hour PI treatment. A) Caspase 3 B) Bcl-2 C) The relationship between Bcl-2 and Bax D) pBad. Data presented as mean \pm SEM. *PI* – *protease inhibitor*.

Next we evaluated the effect of PIs on NOGPs *in vitro*. No significant differences were observed for all four pathways investigated (Figure 3).

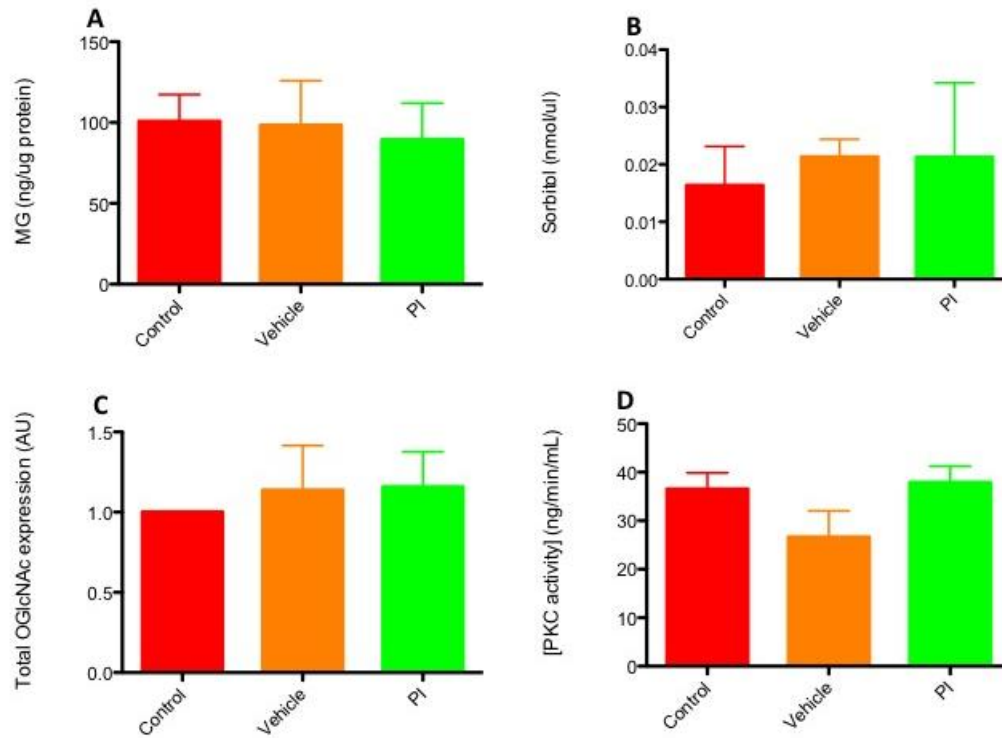


Figure 3. NOGP analysis in rat-derived H9c2 cardiomyoblasts following PI treatment. A) AGE pathway, B) Polyol pathway, C) HBP, D) PKC pathway. Data presented as mean \pm SEM. *PI* – *protease inhibitor*.

Discussion

A significant increase in PI-induced mitochondrial ROS was observed in rat-derived cardiomyoblasts treated with 240 µg/ml Lopinavir/Ritonavir for 24 hours (Figure 1). This is in agreement with other studies showing increased ROS generation with PI treatment in cardiomyocytes³². Here the PI dosage is higher but the treatment time is shorter than in our study, yet notable increases in ROS are observed. Future studies could thus employ a similar model as the latter to ascertain whether NOGP induction occurs at an earlier time point. Nevertheless, we used this concentration of PI for all subsequent cell culture experiments when investigating apoptosis.

No significant changes in apoptosis were observed in PI-treated rat-derived cardiomyoblasts (Figure 2). In agreement, Jiang *et al.*³³ found that ARV treatment of human umbilical cord endothelial cells caused increases in ROS along with mitochondrial dysfunction but did not induce apoptosis, even after 48 hours. A proposed mechanism is due to the mitochondrion's dual function in ROS generation and apoptosis and that ROS-induced mitochondrial dysfunction may thus disrupt its role in cell death.

Changes in NOGP flux were negligible for all four pathways investigated. Here we employed a PI dose and duration that significantly increased the amount of mitochondrial ROS produced. We are unclear how to explain these data but propose that a temporal study should be undertaken to gain additional insights in this regard. Here it would be useful to investigate whether NOGPs may be induced earlier or later in response to PI exposure. Therefore the possibility exists that our 24-hour time point may have 'missed' any NOGP induction that could have occurred. Conversely, this induction may not have

occurred and we need to expose the cells to PIs for a longer time period, e.g. 48 hours. These are now ongoing studies in our laboratory. Another possibility is that the NOGPs do not play a role in these experimental models, and that it is not a downstream target of ROS. The experiments suggested here may shed light on this possibility as well.

Therefore it is evident that while PIs do induce significant increases in mitochondrial ROS in rat-derived cardiomyoblasts, the effects on apoptosis and NOGPs are inappreciable. In future, a wider variety of ROS sources should be also evaluated in order to ascertain the exact effects of PIs on ROS generation *in vitro*. For example, we only focused on mitochondrial-generated ROS and it would be useful to check extra-mitochondrial ROS sources (e.g. NOX) and also RNS. It may also be worthwhile to investigate apoptosis in tissues as well in order to elucidate whether apoptosis would occur following a prolonged treatment period.

Conclusion

In conclusion, our *in vitro* study demonstrates that notable increases in mitochondrial ROS occur following PI treatment but that this is unrelated to increases in cell death or NOGP induction. We therefore propose further investigation into alternative ROS sources as well as apoptotic markers in both cells and tissues generated from *in vivo* experimental models.

References

1. Pieczenik, S. R. & Neustadt, J. Mitochondrial dysfunction and molecular pathways of disease. *Exp. Mol. Pathol.* **83**, 84–92 (2007).
2. Lesnefsky, E. J., Moghaddas, S., Tandler, B., Kerner, J. & Hoppel, C. L. Mitochondrial dysfunction in cardiac disease: ischemia--reperfusion, aging, and heart failure. *J. Mol. Cell. Cardiol.* **33**, 1065–89 (2001).
3. Ballinger, S. W. Mitochondrial dysfunction in cardiovascular disease. *Free Radic. Biol. Med.* **38**, 1278–95 (2005).
4. Chance, B., Sies, H. & Boveris, H. Hydroperoxide metabolism in mammalian organs. *Physiol Rev* **59**, 527–605 (1979).
5. Zaera, Â., Cardellach, F., Casademont, J. & Nunes, V. Mitochondrial involvement in antiretroviral therapy- related lipodystrophy. *AIDS* 1643–1651 (2001).
6. Akki, A., Zhang, M., Murdoch, C., Brewer, A. & Shah, A. NADPH oxidase signaling and cardiac myocyte function. *J Mol Cell Cardiol* **47**, 15–22 (2009).
7. Lagathu, C. *et al.* Some HIV antiretrovirals increase oxidative stress and alter chemokine, cytokine or adiponectin production in human adipocytes and macrophages. *Antivir. Ther.* **12**, 489–500 (2007).
8. Chandra, S., Mondal, D. & Agrawal, K. C. HIV-1 protease inhibitor induced oxidative stress suppresses glucose stimulated insulin release: protection with thymoquinone. *Exp Biol Med* **234**, 442–453 (2009).
9. Touzet, O. & Philips, A. Resveratrol protects against protease inhibitor-induced reactive oxygen species production, reticulum stress and lipid raft perturbation. *AIDS* **24**, 1437–1447 (2010).
10. Ben-Romano, R. *et al.* Nelfinavir induces adipocyte insulin resistance through the induction of oxidative stress: differential protective effect of antioxidant agents. *Antivir. Ther.* **11**, 1051–1060 (2006).
11. Wang, X. *et al.* Human immunodeficiency virus protease inhibitor ritonavir inhibits cholesterol efflux from human macrophage-derived foam cells. *Am. J. Pathol.* **171**, 304–14 (2007).
12. Wang, X., Chai, H., Lin, P. H., Yao, Q. & Chen, C. Roles and mechanisms of human immunodeficiency virus protease inhibitor ritonavir and other anti-human immunodeficiency virus drugs in endothelial dysfunction of porcine pulmonary arteries and human pulmonary artery endothelial cells. *Am J Pathol* **174**, 771–781 (2009).
13. Conklin, B. S. *et al.* HIV protease inhibitor ritonavir decreases endothelium-dependent vasorelaxation and increases superoxide in porcine arteries. *Cardiovasc Res* **63**, 168–175 (2004).
14. Pierce, G. B., Parchment, R. E. & Lewellyn, A. L. Hydrogen peroxide as a mediator of programmed cell death in the blastocyst. *Differentiation* **46**, 181–186 (1991).

15. Watson, R. W., Rotstein, O. D., Jimenez, M., Parado, J. & Marshall, J. C. Augmented intracellular glutathione inhibits Fas-triggered apoptosis of neutrophils. *Blood* **89**, 4175–4181 (1997).
16. Boehning, D. *et al.* Cytochrome c binds to inositol (1,4,5) trisphosphate receptors, amplifying calcium-dependent apoptosis. *Nat. Cell Biol.* **5**, 1051–61 (2003).
17. Sloand, E.M., *et al.* Human immunodeficiency virus type 1 protease inhibitor modulates activation of peripheral blood CD4(+) T cells and decreases their susceptibility to apoptosis in vitro and in vivo. *Blood* **76**, 5966–5973 (1999).
18. Weichold, F. F., *et al.* HIV-1 protease inhibitor ritonavir modulates susceptibility to apoptosis of uninfected T cells. *J Hum Virol* **2**, 261–269 (1999).
19. Matarrese, P., *et al.* Mitochondrial membrane hyperpolarization hijacks activated T lymphocytes toward the apoptotic-prone phenotype: homeostatic mechanisms of HIV protease inhibitors. *J Immunol* **170**, 6006–6015 (2003).
20. Solary, E., Dubrez, L. & Eymin, B. The role of apoptosis in the pathogenesis and treatment of diseases. *Eur. Respir. J.* **9**, 1293–1305 (1996).
21. Terai, C., Kornbluth, R. S., Pauza, C. D., Richman, D. D. & Carson, D. a. Apoptosis as a mechanism of cell death in cultured T lymphoblasts acutely infected with HIV-1. *J. Clin. Invest.* **87**, 1710–5 (1991).
22. Banda, B. N. K. *et al.* Crosslinking CD4 by Human Immunodeficiency Virus gp120 Primes T Cells for Activation-induced Apoptosis. *J Exp Med* **176**, 1099–1106 (1992).
23. Nicholson, D. W. & Thornberry, A. Caspases: killer proteases. *Science* (80-.). **22**, 299–306 (1997).
24. Cory, S. & Adams, J. M. The Bcl2 family: regulators of the cellular life-or-death switch. *Nat. Rev. Cancer* **2**, 647–56 (2002).
25. Mikhailov, V. *et al.* Bcl-2 prevents Bax oligomerization in the mitochondrial outer membrane. *J. Biol. Chem.* **276**, 18361–74 (2001).
26. Datta, S. R., *et al.* 14-3-3 proteins and survival kinases cooperate to inactivate BAD by BH3 domain phosphorylation. *Mol Cell* **6**, 41–51 (2000).
27. Virdee, K., Parone, P. A. & Tolkovsky, A. M. Phosphorylation of the pro-apoptotic protein BAD on serine 155, a novel site, contributes to cell survival. *Curr Biol* **10**, R883 (2000).
28. Strack, P. R., *et al.* Apoptosis mediated by HIV protease is preceded by cleavage of Bcl-2. *Proc Natl Acad Sci USA* **93**, 9571–9576 (1996).
29. Robinson, K. M. *et al.* Selective fluorescent imaging of superoxide in vivo using ethidium-based probes. *Proc. Natl. Acad. Sci. U. S. A.* **103**, 15038–43 (2006).
30. Brown, M. & Wittwer, C. Flow Cytometry: Principles and Clinical Applications in Hematology. *Clin. Chem.* **26**, 1221–1229 (2000).

31. Deng, W., Baki, L., Yin, J., Zhou, H. & Baumgarten, C. M. HIV protease inhibitors elicit volume-sensitive Cl⁻ current in cardiac myocytes via mitochondrial ROS. *J. Mol. Cell. Cardiol.* **49**, 746–52 (2010).
32. Deng, W., Baki, L., Yin, J., Zhou, H. & Baumgarten, C. M. HIV protease inhibitors elicit volume-sensitive Cl⁻ current in cardiac myocytes via mitochondrial ROS. *J Mol Cell Cardiol* **49**, 746–752 (2010).
33. Jiang, B. et al. HIV antiretroviral drug combination induces endothelial mitochondrial dysfunction and reactive oxygen species production, but not apoptosis. *Toxicol Appl Pharmacol* **224**, 60–71 (2007).

Chapter 3

**Analysis of the non-oxidative glucose pathways (NOGP)
following protease inhibitor treatment (*in vivo* generated
samples)**

Introduction

PIs form an integral part of HAART and are highly effective in suppressing viral load in HIV-infected patients. However, long-term therapy often leads to the development of numerous side-effects. For example, Lopinavir/Ritonavir usage causes diarrhea, nausea, and lipid abnormalities such as elevated cholesterol and triglycerides¹. Furthermore, the metabolic alterations associated with PIs largely resemble the MetS, a combination of risk factors leading to future onset of T2DM and CVD². Exacerbation of the MetS phenotype also leads to an increase in cardiovascular complications and IR³ amongst infected individuals, further increasing the disease burden.

Various studies on cell-⁴⁻⁶, animal-⁷⁻⁹ and human-based¹⁰⁻¹⁶ models demonstrated increased plasma cholesterol and triglyceride levels, lipodystrophy and IR as the most common metabolic perturbations with PI usage. Collectively, these serious adverse effects lead to the development of inflammation, stressing the myocardium and eventually progressing to IR and cardiac dysfunction^{14,17}.

Since PIs induce alterations in glucose metabolism, the aim of this study was to determine whether these changes affect regulation of the NOGPs. As before, we again propose increases in NOGP flux as a potential mechanism for PI-induced elevated ROS levels. The same four pathways investigated previously *in vitro* (Chapter 2) will be assessed, i.e. the polyol pathway, HBP, AGE pathway and PKC pathway. Here heart and liver tissues from two separate rat models utilizing PI therapy were utilized to investigate our hypothesis.

Materials and Methods

Protein extraction

We employed tissues collected from two models of PI treatment of rats, i.e. by a) osmotic mini-pump utilization (developed by Dr. Kathleen Reyskens¹⁸), and b) jelly administration (completed by Mr. Burger Symington in our department). For the osmotic mini-pump method, male Wistar rats were subjected to physiologically relevant dose of Lopinavir/Ritonavir (i.e. 7.1 ± 2.9 $\mu\text{g/mL}$) via a mini-osmotic pump for a period of 8 weeks, whereas for the jelly-based method, 44 mg/kg body weight dose of Lopinavir/Ritonavir was dissolved in jelly and administered orally for a period of 16 weeks. This latter dosage was determined after body surface area (BSA) conversion, according to Reagan-Shaw *et al*¹⁹. At the end of the respective treatment periods, rats were sacrificed and cardiac and hepatic tissues were harvested from both animal models. Experimental groups for Group A are as follows: control rats underwent mock surgery, vehicle rats received a mini-osmotic pump containing only ethanol whereas treatment rats received a PI-containing pump for a total of 8 weeks (n=8 per group). For Group B, control rats received no intervention, vehicle rats received only jelly whereas treatment rats received jelly infused with PIs (n=6 per group). The use of animals and procedures were reviewed and approved by the Animal Research Ethics Committee of the Faculty of Natural Sciences of Stellenbosch University (Group A: application numbers 2006B02006, 11NF_REY01, SU_ACUM11_00006, and related amendments, and Group B: application numbers SU_ACUM11_00007A and related amendments). This study adheres to the guidelines set out by the National Institutes of Health's *Guide for the Care and Use of Laboratory*

Animals and performed with the approval of the Animal Ethics Committee of Stellenbosch University (South Africa).

Collected rat tissues (heart and liver) were homogenized in RIPA buffer (50 mM Tris-HCl pH 7.4, 150 mM NaCl, 1% Triton x-100, 1% Sodium deoxycholate, 0.1% SDS, 1 mM EDTA) and centrifuged twice at $7500 \times g$ for 10 minutes. The resultant supernatant was collected as the cytosolic protein fraction. Protein concentration was determined by employing the Bradford technique, with BSA as the protein standard.

Hexosamine biosynthetic pathway

Western blotting analysis (as previously described in Chapter 2) was employed to determine total *O*-GlcNAc expression as a marker for HBP activation.

Advanced glycation end product (AGE) pathway

Methylglyoxal (MG) concentrations were measured by means of a commercial kit (OxiSelect™ MG ELISA Kit; Cell Biolabs, San Diego CA) to assess AGE pathway activation (as previously described in Chapter 2).

Protein kinase C (PKC) pathway

The PKC assay was carried out using an ELISA-based commercially available kit (Enzo Life Sciences, Farmingdale NY) and protocol was followed as detailed in the kits instruction manual (as previously described in Chapter 2).

Polyol pathway

D-sorbitol levels were measured as detailed in the instructions of a commercially obtained kit (BioVision K 631-100, Mountain View CA), as previously described in Chapter 2.

Statistical analysis

Statistical analysis was performed by one-way ANOVA and the Bonferroni *post-hoc* test was used to determine differences between groups (GraphPad Prism v5, San Diego CA).

Data are presented as mean \pm SEM, and values considered significant when $p < 0.05$.

Results

The results from both rat models are presented grouped per tissue type (heart, liver), per pathway investigated. Hereafter the 8-week group (mini-osmotic pump administration) will be referred to as Group A and the 16-week group (jelly-based administration) as Group B. Group A consisted of n=8 rats per experimental group whereas Group had n=6 rats per experimental group.

For the AGE pathway we observed a significant decrease in MG in the liver of Group A rats but not in Group B rats (Figure 1). Here PI treatment decreased MG levels to 13.63 ± 2.624 ng/ μ g protein vs. control 31.88 ± 6.607 ng/ μ g protein ($p < 0.01$); and vs. vehicle 34.22 ± 3.723 ng/ μ g protein ($p < 0.01$).

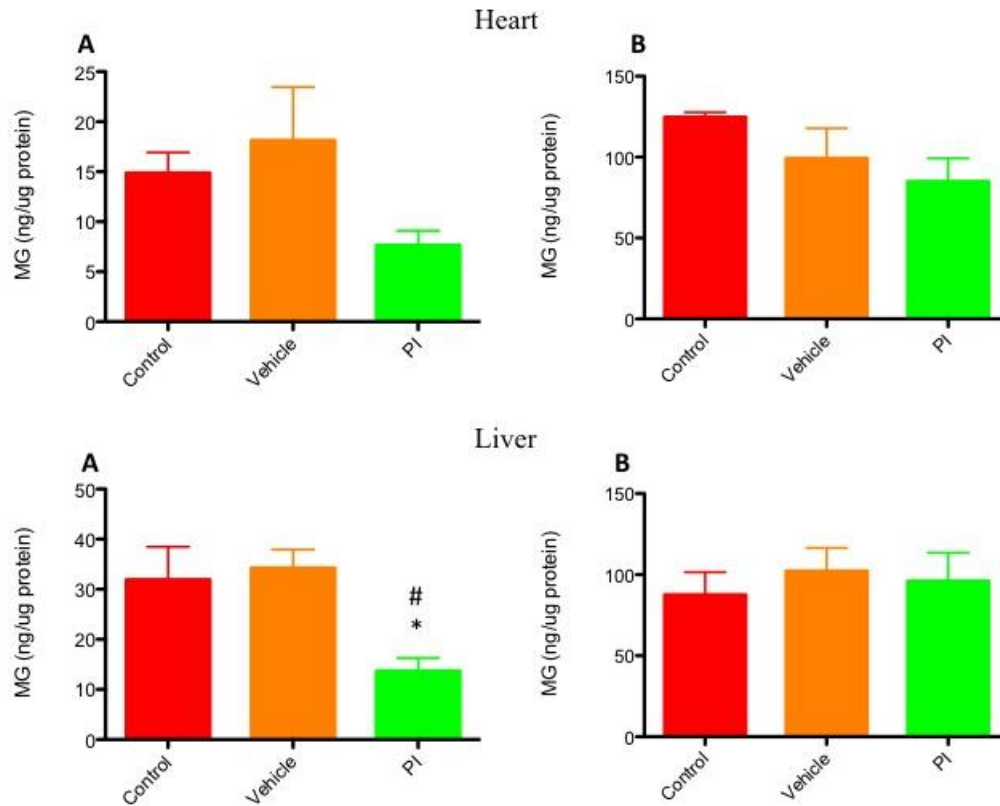


Figure 1. AGE pathway analysis in the rat heart and liver following PI treatment. Results are presented as the amount of MG produced per μg protein in the sample. Group A results are presented on the left and Group B on the right, for liver and heart respectively. Data presented as mean \pm SEM. * $p < 0.01$ vs. Control, # $p < 0.01$ vs. Vehicle. PI – protease inhibitor.

Next sorbitol levels were assessed as marker of polyol pathway induction. No significant differences were observed between groups.

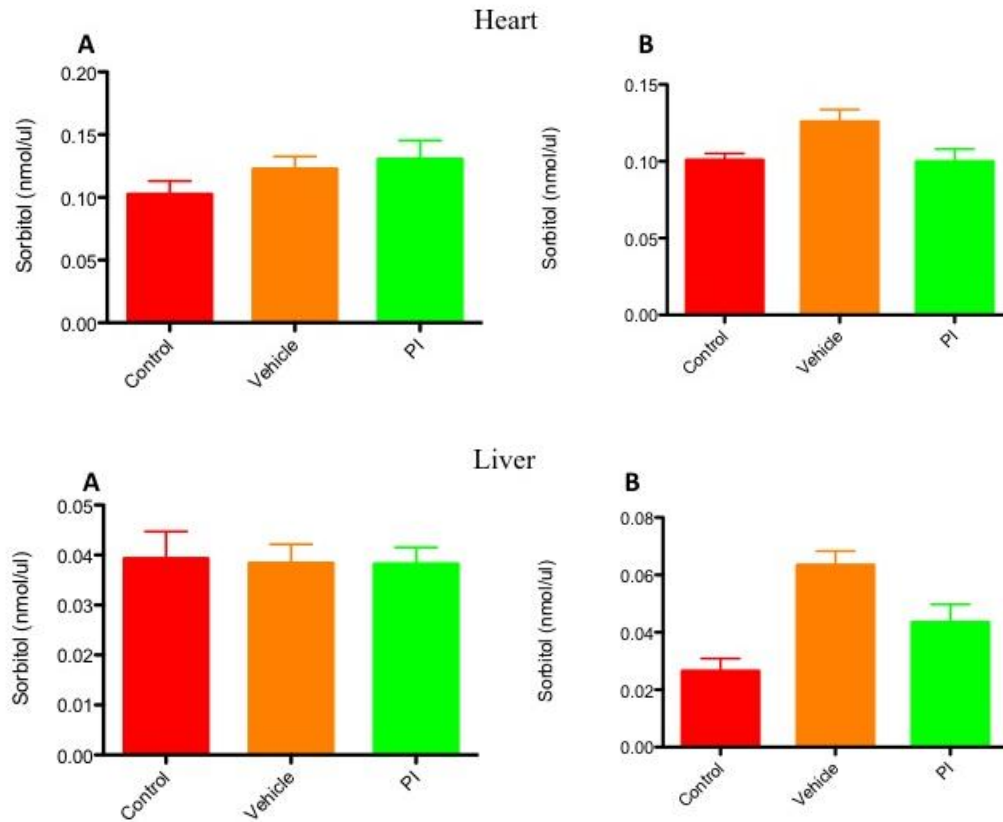


Figure 2. Polyol pathway analysis in the rat heart and liver following PI treatment. Results are presented as the amount of sorbitol produced per μL protein in the sample. Group A results are presented on the left and Group B on the right, for liver and heart respectively. Data presented as mean \pm SEM. *PI* – protease inhibitor.

The HBP pathway was next investigated but no significant differences were observed between groups.

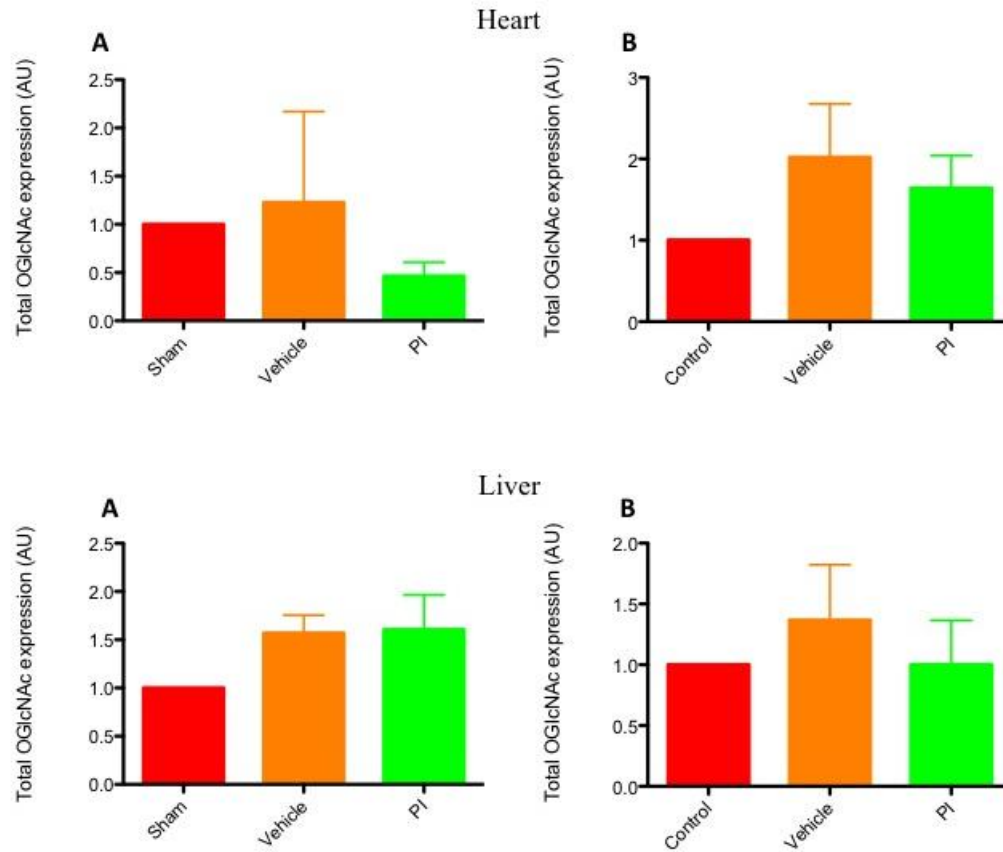


Figure 3. HBP pathway analysis in the rat heart and liver following PI treatment. Results are presented as the amount of *O*-GlcNAc normalized to β -actin. Group A results are presented on the left and Group B on the right, for liver and heart respectively. Data presented as mean \pm SEM. *PI* – *protease inhibitor*.

Finally, the PKC pathway was investigated. Once again no significant differences were observed between groups.

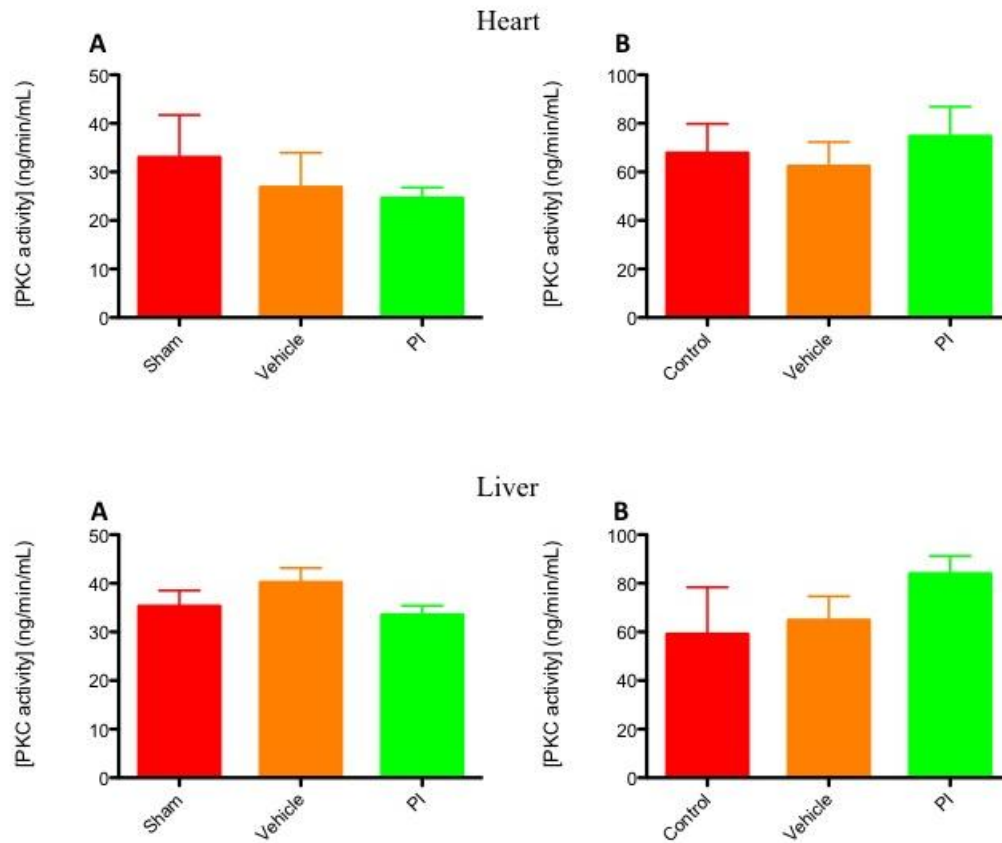


Figure 4. PKC pathway analysis in the rat heart and liver following PI treatment. Results are presented as the amount of PKC kinase activity observed. Group A results are presented on the left and Group B on the right, for liver and heart respectively. Data presented as mean \pm SEM. *PI* – *protease inhibitor*.

Discussion

Significant down-regulation of the AGE pathway was observed in the liver of Group A. To further elucidate the cause of this observation, separate experiments were performed (by Dr. Kathleen Reyskens¹⁸) to assess the total, free and oxidized GSH levels. Here the rationale was based on studies by Lander *et al.*²⁰ on rat pulmonary artery smooth muscle cells that showed depletion of intracellular GSH resulted in increased sensitivity of cells to AGE-mediated pathway induction. We therefore expected that the converse would be valid: an increase in intracellular GSH would allow for a decrease in AGE-mediated pathway induction. However, results for this study remain inconclusive as no significant changes were observed in GSH levels in tissues (data not shown).

For the rest of the pathways investigated, no significant differences were observed between experimental groups. For Group A we attribute this to the duration of exposure to PIs, i.e. eight weeks might not be long enough for PIs to induce changes in the NOGPs. Most human-based studies highlighting the adverse effects of PIs employ a treatment period of more than six months^{21–24}. However, the longer treatment period for Group B also did not result in any significant changes. Although changes to the NOGP flux are not significant, the data suggest that the level of pathway induction for Group B is higher than Group A in some instances. For example, the amount of MG produced in the heart and liver of Group B rats is higher than Group A (Figure 1). A similar trend exists for the rest of the pathways investigated (Figure 2-4). However, the jelly-based model resulted in a less severe phenotype than the mini-osmotic pump method. For example, the mini-osmotic pump method elicited several metabolic changes after 8 weeks²⁵ while the jelly-

based method did not (Symington, unpublished data). This may be the case since the mini-osmotic pump delivers PIs at a steady rate and in a continuous fashion, while the jelly-based method only delivers the PIs at specific times (when ingested). This may help explain why 8 weeks by the mini-osmotic pump results in a more severe phenotype. Therefore increasing the duration of exposure to PI treatment – especially with the mini-osmotic pump model - may result in more conclusive evidence for NOGP induction in future. However, further studies are required to test whether this is indeed the case.

Another concern for the jelly-based method (Group B) is that it contains ingredients that can adversely affect experimental results. For example, according to Coleman and Anderson²⁶, the original formulation for jelly-type confections contains sorbitol as an alternative sweetener. In agreement, our results for polyol pathway induction in Group B show higher sorbitol levels when compared to the control (Figure 2), especially in the liver. Thus the vehicle utilized may negatively affect results for Group B and future studies should consider an alternative vehicle for drug administration.

Conclusion

In conclusion, our study demonstrates that PI exposure does not activate NOGPs, suggesting that these pathways are not detrimental in terms of cardio-metabolic dysfunction found with PIs. However, the liver exhibited lower AGE pathway activation that needs more studies to clarify its significance in terms of metabolic dysfunction found in this model (mini-osmotic pump). We propose future studies with modifications to the current rat models in order to evaluate the effects of PIs on the NOGPs.

References

1. Hawkins, T. Understanding and managing the adverse effects of antiretroviral therapy. *Antiviral Res.* **85**, 201–9 (2010).
2. Reaven, G. *The metabolic syndrome*. 11–36 (Humana Press, 2008).
3. Carr, A. *et al.* A syndrome of peripheral lipodystrophy, hyperlipidaemia and insulin resistance in patients receiving HIV protease inhibitors. *AIDS* **12**, F51–58 (1998).
4. Hruz, P. W., Yan, Q., Struthers, H. & Jay, P. Y. HIV protease inhibitors that block GLUT4 precipitate acute, decompensated heart failure in a mouse model of dilated cardiomyopathy. *FASEB* **22**, 2161–2167 (2008).
5. Hruz, P. HIV protease inhibitors and insulin resistance: lessons from in vitro, rodent and healthy human volunteer models. *Diabetes* **3**, 660–665 (2009).
6. Murata, H., Hruz, P. W. & Mueckler, M. Indinavir inhibits the glucose transporter isoform Glut4 at physiologic concentrations. *AIDS* **16**, 859–863 (2002).
7. Liang, J.-S. *et al.* HIV protease inhibitors protect apolipoprotein B from degradation by the proteasome: A potential mechanism for protease inhibitor-induced hyperlipidemia. *Nat Med* **7**, 1327–1331 (2001).
8. Parker, R. A. *et al.* Endoplasmic reticulum stress links dyslipidemia to inhibition of proteasome activity and glucose transport by HIV protease inhibitors. *Mol Pharmacol* **67**, 1909–1919 (2005).
9. Behrens, G. *et al.* Impaired glucose tolerance, beta cell function and lipid metabolism in HIV patients under treatment with protease inhibitors. *AIDS* **13**, F63–70 (1999).
10. Bastard, J. *et al.* Association between altered expression of adipogenic factor SREBP1 in lipoatrophic adipose tissue from HIV-1-infected patients and abnormal adipocyte differentiation and insulin resistance. *Lancet* **359**, 1026–1031 (2002).
11. Carr, A. *et al.* HIV protease inhibitor substitution in patients with lipodystrophy: a randomized, controlled, open-label, multicentre study. *AIDS* **15**, 1811–1822 (2001).
12. Dong, K. *et al.* Changes in body habitus and serum lipid abnormalities in HIV-positive women on highly active antiretroviral therapy (HAART). *J AIDS* **21**, 107–113 (1999).
13. Gan, S. *et al.* Altered myocellular and abdominal fat partitioning predict disturbance in insulin action in HIV protease inhibitor-related Lipodystrophy. *Diabetes* **51**, 3163–3169 (2002).
14. Tsiodras, S., Mantzoros, C., Hammer, S. & Samore, M. Effects of protease inhibitors on hyperglycemia, hyperlipidemia, and lipodystrophy: a 5-year cohort study. *Arch Intern Med* **160**, 2050–2056 (2000).
15. Floris-Moore, M. *et al.* Increased serum lipids are associated with higher CD4 lymphocyte count in HIV-infected women. *HIV Med* **7**, 421–430 (2006).

16. Rudich, A., Ben-Romano, R., Etzion, S. & Bashan, N. Cellular mechanisms of insulin resistance, lipodystrophy and atherosclerosis induced by HIV protease inhibitors. *Acta Physiol Scand* **183**, 75–88 (2005).
17. Behrens, G. M. N. et al. Impaired glucose phosphorylation and transport in skeletal muscle cause insulin resistance in HIV-1 – infected patients with lipodystrophy. *J Clin Invest* **110**, 1319–1327 (2002).
18. Reyskens, K. M. S. E. The Maladaptive Effects of HIV Protease Inhibitors (Lopinavir/Ritonavir) on the Rat Heart. 27 (2013).
19. Reagan-Shaw, S., Nihal, M. & Ahmad, N. Dose translation from animal to human studies revisited. *FASEB J.* **22**, 659–61 (2008).
20. Lander, H. M. Activation of the Receptor for Advanced Glycation End Products Triggers a p21ras-dependent Mitogen-activated Protein Kinase Pathway Regulated by Oxidant Stress. *J. Biol. Chem.* **272**, 17810–17814 (1997).
21. Mary-Krause, M., Cotte, L., Simon, A., Partisani, M. & Costagliola, D. Increased risk of myocardial infarction with duration of protease inhibitor therapy in HIV-infected men. *AIDS* **17**, 2479–86 (2003).
22. Carr, A. et al. Diagnosis, prediction, and natural course of HIV-1 protease-inhibitor-associated lipodystrophy, hyperlipidaemia, and diabetes mellitus: a cohort study. *Lancet* **353**, 2093–2099 (1999).
23. Periard, D. et al. Atherogenic Dyslipidemia in HIV-Infected Individuals Treated With Protease Inhibitors. *Circulation* **100**, 700–705 (1999).
24. Van der Valk, M. et al. Lipodystrophy in HIV-1-positive patients is associated with insulin resistance in multiple metabolic pathways. *AIDS* **15**, 2093–100 (2001).
25. Reyskens, K. M. S. E. et al. The Maladaptive Effects of HIV Protease Inhibitors (Lopinavir/Ritonavir) on the Rat Heart. *PLoS One* **8**, e73347 (2013).
26. Coleman, E. C. & Anderson, N. E. Shelf-stable Gelled Confections. 3–5 (1994).